Nano Energy 103 (2022) 107762

Contents lists available at ScienceDirect

Nano Energy

journal homepage: www.elsevier.com/locate/nanoen

Applications of nanogenerator-based wearable devices in orthopedics

Dengjie Yu [a,c,e,1], Zhe Li [b,c,1], Wenqing Xie [a,e], Daishi Li [d], Zhou Li [c,f,*], Yusheng Li [a,e,**]

[a] Department of Orthopedics, Xiangya Hospital, Central South University, Changsha 410008, China
[b] School of Medical Technology, Institute of Engineering Medicine, Beijing Institute of Technology, Beijing 100081, China
[c] Beijing Institute of Nanoenergy and Nanosystems, Chinese Academy of Sciences, Beijing 101400, China
[d] Department of Dermatology, Xiangya Hospital, Central South University, Changsha 410008, China
[e] National Clinical Research Center for Geriatric Disorders, Xiangya Hospital, Central South University, Changsha 410008, China
[f] School of Nanoscience and Technology, University of Chinese Academy of Sciences, Beijing 100049, China

ARTICLE INFO

Keywords:
Nanogenerator
Self-powered
Wearable devices
Orthopedics

ABSTRACT

As an important part of internet of things (IOTs), wearable devices can provide real time monitoring for each individual and have shown the potential in personalized medical treatment. Orthopedics is an important branch of surgery and it focus on the injuries and disorders of musculoskeletal system. With the acceleration of population aging, the incidence of both chronic and acute orthopedics diseases is increasing, leading to significant public health and economic burden. Wearable devices have broad application prospects in diagnosis, treatment and post-rehabilitation monitoring of orthopedic diseases. However, batteries have limitations of inconvenient charging, service life, which greatly hinder the long-term applications of wearable devices. As a positive energy conversion device, nanogenerators (NGs) can convert the biomechanical energy generated by daily activities into electricity. The device can be applied not only for energy supply, but also as a self-powered sensor. This review concludes the working principles and material design strategies of several kinds of NGs, summarizes the applications of nanogenerator-based (NG-based) wearable devices in orthopedics, and prospects the opportunities and challenges that such devices will face in the future. This review may inspire further development of NG-based wearable devices and their applications in orthopedics.

1. Introduction

Orthopedics is a branch of surgery that focus on treating the injuries and disorders of musculoskeletal system, including skeletal muscle, bone, spine, cartilage, soft tissues like ligaments, joints like knee, hip, ankle, shoulder. The subspecialties of orthopedics are very versatile. In general, they can be divided into sports medicine, deformity correction, injury/fracture treatment, and musculoskeletal infection or oncology treatment [1]. Though orthopedics is considered as a subspecialty of surgery, non-surgical management is of equal importance to surgical management, no matter in acute injuries or chronic disorders [2,3]. Non-surgical management has been shown to be critical in early intervention, chronic diseases treatment and post-operative rehabilitation [3–5].

Recently, personalized medicine has received much attention in orthopedics, especially personalized non-surgical intervention. Depending on each individual condition, different clinical treatment strategies are considered by doctors. However, the promotion of personalized medicine is difficult because disease condition is not static. Either improved or deterioration, strategies should be adjusted. But once discharged, doctors are unable to obtain information on disease progression in time, causing medical cost increase and overtreatment [6]. Internet of things (IoTs), which is a network linking every objective. now is extensively used in healthcare. Wearable devices are one of the important parts in IoTs. They can provide easily obtainable healthcare for patients and decentralized healthcare center from hospitals to homes [7]. Now there are many wearable devices have been applied into healthcare monitoring, including dynamic biofluids measurement [8], cardiovascular monitoring [9] and respiration monitoring [10]. But the biggest obstacle to make wearable biosensors for long-term use is power limitation. Though batteries can fulfill most demands of wearable devices, the limitations are obvious at the same time, such as limited endurance,

* Corresponding author at: Beijing Institute of Nanoenergy and Nanosystems, Chinese Academy of Sciences, Beijing 101400, China.
** Corresponding author at: Department of Orthopedics, Xiangya Hospital, Central South University, Changsha 410008, China.
E-mail addresses: zli@binn.cas.cn (Z. Li), liyusheng@csu.edu.cn (Y. Li).
[1] These authors contributed equally to this work.

https://doi.org/10.1016/j.nanoen.2022.107762
Received 18 July 2022; Received in revised form 18 August 2022; Accepted 30 August 2022
Available online 5 September 2022

need to recharge, and environmental pollution [11]. Nanogenerators (NGs) is a kind of self-powered devices which can convert mechanical energy into electricity. Compared with electromagnetic induction, NGs are better at collecting low-frequent mechanical energy and presented a great potential in harvesting distributed energy [12]. In addition, the output signals can reflect the extent of movement, which meets the needs in orthopedics applications [13]. Here, the recent progress of nanogenerators in orthopedics are summarized, and the challenge and prospective are discussed (Fig. 1). Firstly, the working mechanism of nanogenerators was introduced. Then, the materials strategies of wearable nanogenerators including textile-based, flexible film and integrated film, and the applications of wearable NGs in orthopedics were discussed. Finally, we listed the limitations and proposed our perspectives for the applications of wearable devices based on NGs in orthopedics.

2. Working principle of nanogenerators

2.1. Triboelectric nanogenerator (TENG)

The phenomenon of making two different objects charged by friction is called triboelectrification. When the two triboelectric layers displace relatively, potential difference between working electrodes will drive electrons flow across, which contributing to the generation of electricity [21,22]. In 2012, Wang et al. firstly demonstrated that low frequency mechanical energy can be converted into electricity by using triboelectric nanogenerator [23]. Because the relative motion of different (even the similar) materials can lead to the electron transfer, almost all

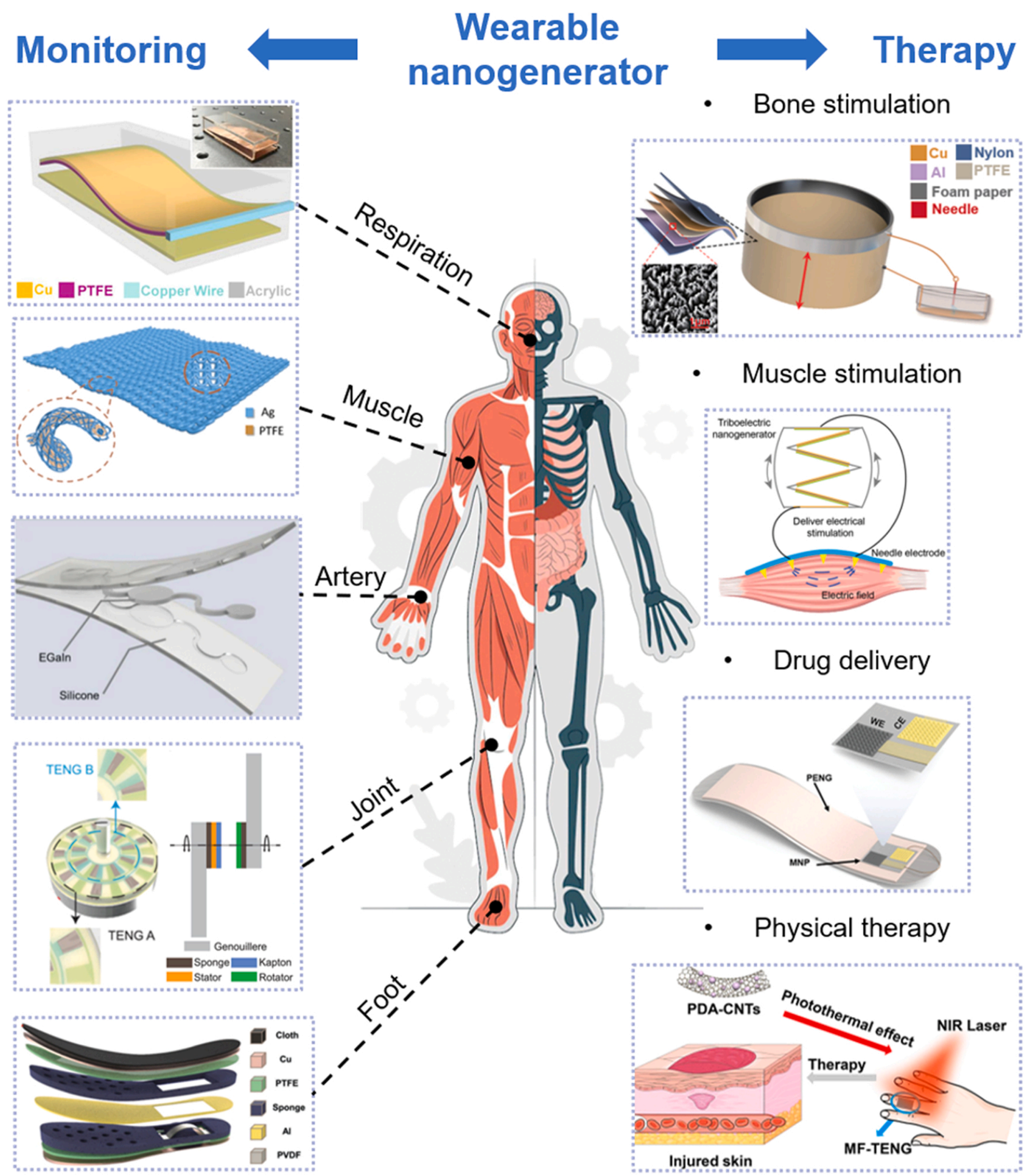

Fig. 1. An overview of NG-based wearable devices in orthopedics. Reproduced with permission [14]. Copyright 2018, American Chemical Society. Reproduced with permission [15]. Copyright 2021, Elsevier Ltd. Reproduced with permission [16]. Copyright 2020, WILEY-VCH Verlag GmbH & Co. KGaA, Weinheim. Reproduced with permission [17]. 2022 Wiley-VCH GmbH. Reproduced with permission [18]. Copyright 2022, Wiley-VCH GmbH. Reproduced with permission [19]. Copyright 2021 Wiley-VCH GmbH. Reproduced with permission [20]. Copyright 2021, American Chemical Society. Designed using images from Freepik.com.

materials in our daily life can be used for the fabrication of TENG. There are four working mechanisms for TENGs, vertical contact-separation mode, lateral sliding mode, single-electrode mode, and freestanding triboelectric-layer mode (Fig. 2a) [24].

2.1.1. Vertical contact-separation mode

Vertical contact-separation mode was first demonstrated by Zhu et al. in 2012. The operating principle of this mode can be summarized as the coupling of electrostatic induction and friction electrification.

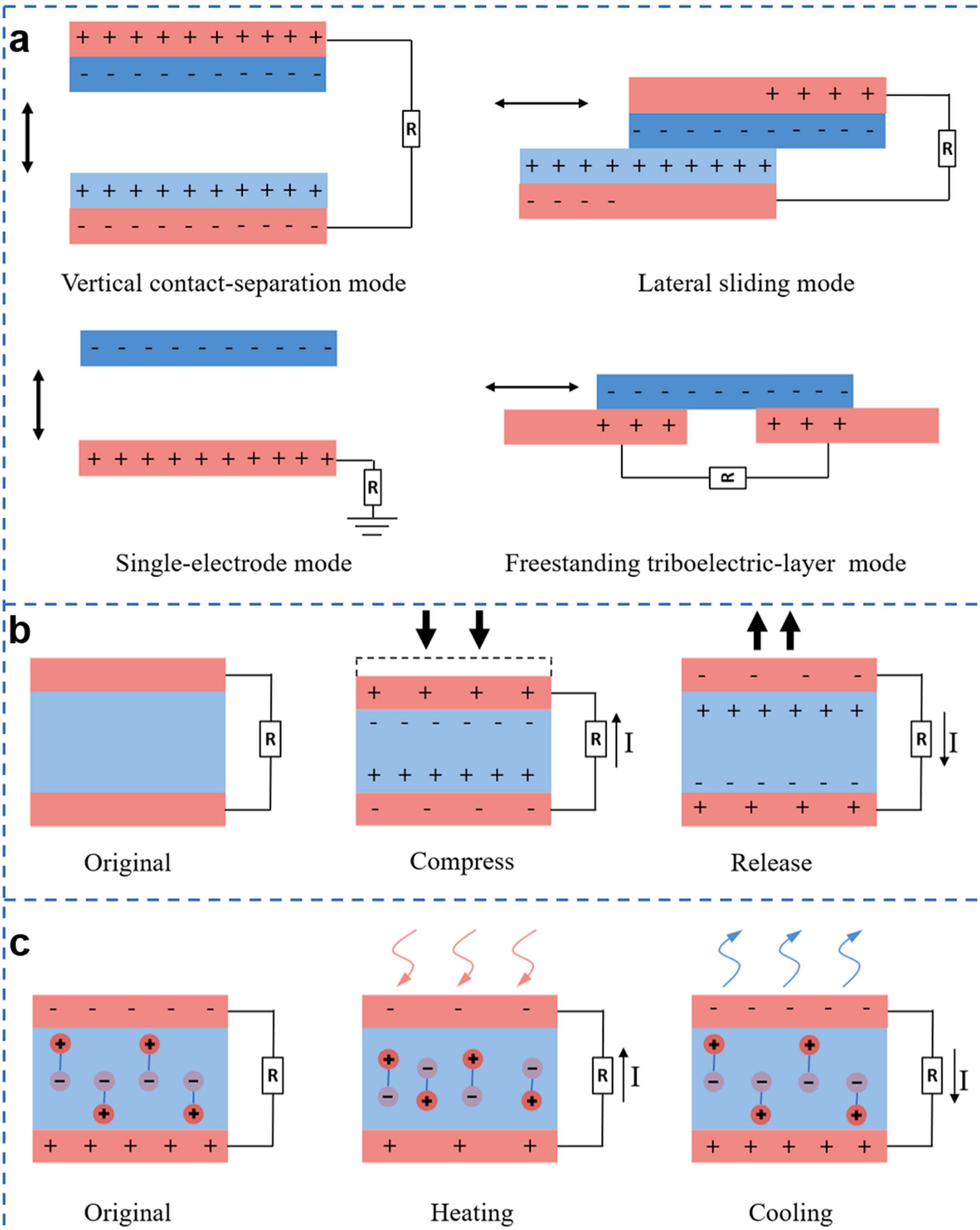

Fig. 2. (a) Four working modes of triboelectric nanogenerator. (b) Working mechanism of piezoelectric nanogenerator. (c) Working principle of pyroelectric nanogenerator.

Contact between two friction layers with different electron affinities will produce opposite induced charges. When the two layers separate, a potential difference will be formed between the electrode layers on the upper and lower surfaces of the friction layer. If the two electrodes are electrically connected through a load, free electrons will flow from one electrode to the other, forming an opposite potential to balance the electrostatic field. When the friction layers contact again, the electron reverse flow. Periodic contact and separation between the two materials drive induced electrons to flow back and forth between the two electrodes, resulting in an alternating current output in the external circuit [25]. The electricity process under vertical contact-separation mode depends on the periodic contact and separation and the output is periodic alternating current.

2.1.2. Lateral sliding mode

The sliding mode is the process that generates triboelectricity and planar charge separation under horizontal force. Driven by the force, the two friction layers slide relatively in the horizontal direction, and frictional electrification generates dense static contact. The contact area on the surface of the two materials changes periodically with the sliding, and an induced potential difference is generated between the two friction layers. Because of the existence of the potential difference, electrons flow between the two electrode layers through the load to offset the difference [26]. There are many structures in this mode, including micro-grating, [27] linear-grating, [28] case-encapsulated, [29] etc. Compared with vertical contact-separation mode, friction layers don't have to separate, which expanded the application horizon of TENGs.

2.1.3. Single-electrode mode

The electrodes of TENGs based on single-electrode mode and lateral sliding mode need to connect to the moving objects and form a closed loop with the external circuit, which extremely restricted the activity scope of friction layers. TENG in single electrode mode requires only one electrode to be connected to the friction layer of Nanogenerator. The other electrode is only a reference electrode for potential, which can be placed arbitrarily or even directly grounded. Therefore, the other electrification surface of TENG in single electrode mode can move freely without electrode restriction. However, the single electrode mode of TENG also has a disadvantage, that is, the overall electrical output is only half of that in the corresponding other mode. When the top friction layer contact with the bottom friction layer, the potential is similar in two layers. Charge balance and there is no potential difference between the friction layer and the ground. Because of the external forces, two layers separated and potential difference generated between ground and electrode, which drives electrons to flow towards the electrode until the maximum clearance is reached [30,31]. The friction layer of this mode can move freely without being connected to the load and broaden the application field.

2.1.4. Freestanding triboelectric-layer mode

TENGs based on freestanding triboelectric-layer mode are composed of two stationary and connected electrodes and a freestanding friction layer parallel to electrodes. With the friction layer sliding between the electrodes, induced charge changes periodically and the potential difference between the two electrodes changes. The potential difference drives electrons flow between two electrodes, resulting in the current flows through external circuit [32]. Common freestanding triboelectric-layer mode types are rolling friction structure, [33] radial-arrayed rotary structure, [34], and linear grating structure [35]. The benefits of this mode are convenient for the devices' design and high energy conversion efficiency. In addition, non-contact movement can occur between the freestanding friction layer and the electrode layers and also has a relatively high output [36].

For the fabrication of wearable devices, selecting proper mechanism is very important, which depends on the purpose of the wearable devices. For TENG, Contact and separation can be occurred during almost all activities. Therefore, the range of application of vertical contact-separation mode is broad. Motions from large-scale joint motion to subtle vascular pulsation can be detected [37]. In addition, it can serve as a power source harvesting energy from physiologic activities for medical stimulation [38]. Lateral sliding mode is suitable for harvesting from cycled movement like respiration [39]. Single-electrode mode is widely applied in human-machine interactions. Skin can be employed as one of the friction layers and more detailed signals can be detected [40]. Free standing mode has shown a high resolution and accuracy in angle sensing [16,41]. By integrating different modes, both output and application fields can be broadened.

2.2. Piezoelectric nanogenerator (PENG)

Piezoelectric material is a kind of crystal material with potential difference between the two faces under pressure, which can realize the mutual conversion of mechanical energy and electric energy. In 2006, Wang et al. first demonstrated the piezoelectric nanogenerator based on zinc oxide (ZnO) nanowire arrays could convert mechanical energy into electricity [42]. Zinc oxide has non-central symmetry wurtzite structure. When external force is applied, positive and negative charge surface will be generated on the material surface, which is called polar surface. The piezoelectric potential generated by these polar surfaces can be used to drive the movement of electrons in the outer circuit and realize the conversion of mechanical energy to electrical energy (Fig. 2b) [43]. Compared with TENG, PENG is more dependent on the piezoelectric effect of the material itself. The materials can be roughly divided into 3 types: organic, inorganic and complex piezoelectric materials. Most representative organic piezoelectric material is polyvinylidene fluoride (PVDF), [44,45] inorganic materials include piezoelectric single crystal and piezoelectric ceramics, [46,47] biological materials, from basic components of body like amino acid and protein to tissues like skin and bone, also have piezoelectricity [48]. Complex piezoelectric materials are different shapes of inorganic piezoelectric materials embedded in organic polymer substrate. Most of piezoelectric materials are flexible and have different structures, which ensure the high output of piezoelectric nanogenerators [49].

2.3. Thermal/pyroelectric nanogenerator

Utilizing thermal energy is promising for power generation. Thermoelectric and pyroelectric are the major methods to convert heat into electricity at present. Both of which have their advantages.

The temperature difference (ΔT) between two sides of thermoelectric materials causes the voltage difference, leading to power generation, which has been applied for self-powered device fabrication [50]. With the exploration and combination of new materials, the thermoelectric conversion efficiency has been improved rapidly [51]. Another point for the thermoelectric effect is the Peltier effect, which indicates that current flow in the thermoelectric materials can lead to ΔT between the two sides. This effect is widely used in the heat or cooling by electricity [52]. At present, thermal nanogenerators-based devices have been shown its potential in medical field [53].

The pyroelectric effect depends on the temperature variation over time, which leads to the change of polarization intensity inside the material. Pyroelectric effect includes basic pyroelectric effect and secondary pyroelectric effect. Without being imposed to external forces, the variation of the temperature leads to the amplitude of electric dipole inside the materials change, which is called pyroelectric effect. Secondary pyroelectric effect means that when the volume of materials changes due to the temperature variation, inducing the piezoelectric effect of materials. Potential difference is generated between the electrode and leads to the electrons directional movement [54,55]. Yang et al. first demonstrated the pyroelectric nanogenerators (PyNG) in 2012. They chose ZnO nanowire as the pyroelectric materials. When the temperature changed, current can be detected in the external circuit

(Fig. 2c) [56].

2.4. Hybrid and coupled nanogenerator

Energy in the environment does not exist in a single form. Hybrid nanogenerators can collect different kinds of energy from environment

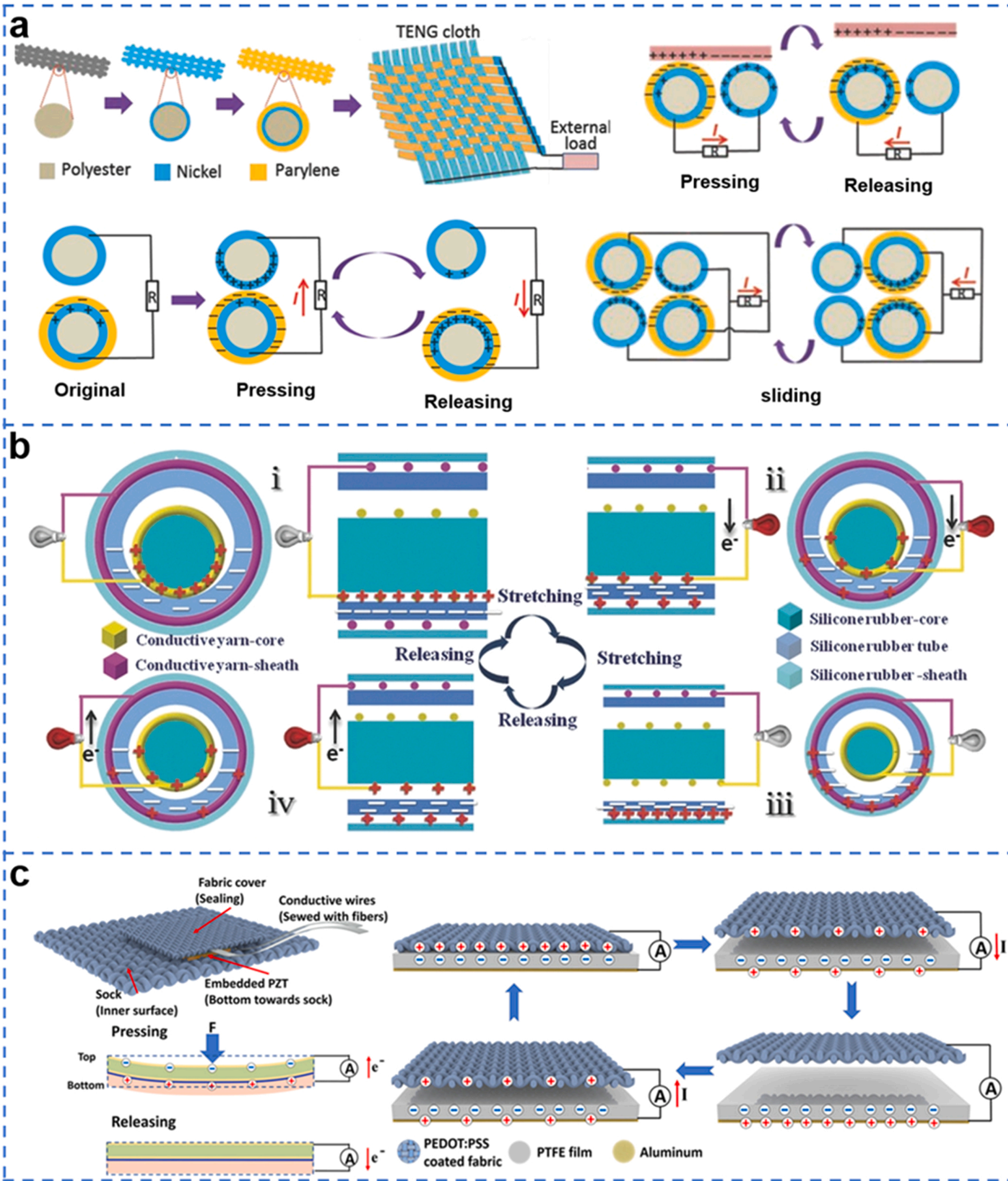

Fig. 3. Different mechanisms of wearable nanogenerators based on textile. (a) Woven-structure TENG cloth based on interweaving nickel cloth and parylene cloth. Reproduced with permission [65]. Copyright 2015, WILEY-VCH Verlag GmbH & Co. KGaA Weinheim. (b) Single yarn based TENG with core-sheath and built-in spring-like spiral winding structures. Reproduced with permission [68]. Copyright 2018, WILEY-VCH Verlag GmbH & Co. KGaA Weinheim. (c) Fabric-based tri-boelectric-piezoelectric hybrid sock. Reproduced with permission [75]. Copyright 2019, American Chemical Society.

at the same time or through different energy conversion mechanism to improve output efficiency. Piezoelectric-triboelectric nanogenerator is the most common kind of hybrid nanogenerator by using piezoelectric materials as triboelectric layer. Singh et al. fabricated a ZnO-PVDF/polytetrafluoroethylene (PTFE) based triboelectric-piezoelectric hybrid nanogenerator (TPNG). PVDF was employed to provide piezoelectric effect. At the same time, the incorporation of ZnO nanorods into the PVDF matrix enhanced both the piezoelectric and triboelectric effects of PVDF, resulting in the instantaneous output power density up to 24.5 μW cm^{-2}. The two different output signals were generated by a single material, which provided a novel approach to improve nanogenerator output [57].

Piezoelectric and pyroelectric effects depend on their own properties of materials. Some materials both have pyroelectric and piezoelectric behaviors. Lee et al. developed a piezoelectric-pyroelectric hybrid nanogenerator (PPNG) based on poly(vinylidenefluoride-co-trifluoroethylene) (P(VDF-TrFE) polymer. They employed polydimethylsiloxane (PDMS)-carbon nanotubes (CNT) composite to provide stretchability and flexibility for the device as well as served as robust electrode on the bottom. In addition, to improve the pyroelectric effect efficiency, graphene was covered as the top electrode for fast temperature gradient [58]. PVDF is a typical material with pyroelectric, piezoelectric and triboelectric behaviors. Several hybridized triboelectric–piezoelectric–pyroelectric nanogenerators (TPPNG) based on PVDF has been developed. Zi et al. developed a multilayered planer structured TPPNG. It was a combination of a TENG and PPNG. They placed a lateral-sliding TENG upon the PPNG, triboelectric layers were composed of PTFE and copper. The piezoelectric and pyroelectric outputs were generated by PVDF. Under a 4.41 Hz sliding frequency, TENG achieved a maximum output of 46.2 mW m^{-2}. The output of PPNG depended on the temperature variation and force exert to the sensor. By integrating TENG and PPNG, energy harvesting efficiency can be enhanced up to 26.2 % [59].

Integrating nanogenerators with other energy harvesting methods can enable optimal output under different conditions. Hybridizing thermal, [60] electromagnetic, [61] biofuel, [62] photovoltaic [63] and many other energies with nanogenerator have been proposed, compensating the deficiency of using nanogenerators only.

3. Materials strategies of wearable nanogenerators

3.1. Textile-based NGs

The integration of textile and nanogenerators best matches the definition of wearable device. Textile-based wearable devices have various advantages, like high stretchability, durability, which have attracted widespread attention [64]. There are three types of textile-based NGs at present (Fig. 3).

The first kind is woven structure NGs. They are fabricated by interweaving different materials into textile. Pu et al. integrated a textile-TENG with lithium-ion battery (LIB) belt. The textile-TENG was fabricated based on polyester substrate. They first coated conductive nickel film on the substrate, called Ni-cloth. Then insulating parylene film on Ni-cloth, fabricating a parylene-cloth. The textile-TENG was fabricated by interweaving Ni-cloth and parylene-cloth, and each cloth was acted as an electrode. It had double work modes, contact-separation mode and lateral sliding mode, which ensured enough output under different motions. The maximum voltage and current were 50 V, 4 μA. The energy generated by TENG was used to charge the LIB belt, resulting in a self-charging power unit for wearable application (Fig. 3a) [65]. Zhou et al. selected nylon fabric and polyester fabric as friction layers as well as conductive silver fiber fabric as electrodes. All materials are common and easily obtained. Then they inter-weaved all materials into a textile. There were two working principles of the device, which were vertical contact-separation mode and freestanding mode respectively, making it suitable to work under deformation and undeformation conditions [66].

The second type is single yarn-based NGs. By weaving yarn NGs into fabric, the fabric also has ability for power generation. Kim et al. developed a fiber-structured TENG (FTENG) by weaving fibers. The fiber consisted 2 parts: i) nanostructured PDMS tube as the shell. ii) Au coated Al wire as the core. Under 50 N, 10 Hz cycled compressive force, the output of a 5 cm fiber was 40 V and 10 μA. No output degradation in high humidity environment. After woven into fabric, under the same force, the FTENG can generate the output of 40 V and 210 μA, instantaneous power output can reach up to 4 mW [67]. Dong developed a core-sheath TENG yarn (Fig. 3b) with and built-in spring-like spiral winding structures [68]. Silver-coated nylon yarn was employed as electrode materials as well as silicone rubber was selected as dielectric, supporting and encapsulating material, which provided the TENG with well mechanical robustness, good biocompatibility and excellent flexibility and stretchability. The TENG consisted of two spring-like spiral winding structured parts, which were the internal core column, and the outer sheath tube. The internal core column was fabricated by the conductive nylon yarn (as the inner electrode) winding around the supporting silicon rubber column. The external sheath tube also fabricated by a conductive nylon yarn (as the outer electrode) and silicone rubber. Nylon yarn was twisted on the surface of silicone rubber tube. Axially inserted internal core column into external sheath tube, the core-sheath TENG was fabricated. The gap of core-sheath structure endows TENG with enough contact-separation space. In addition, spiral structure provided high stretchability and fast response. Under a frequency of 3 Hz, maximum average power densities of TENG can achieve 11 and 0.88 W m^{-3} when compressing and stretching respectively [69]. Ma et al. developed a core-sheath TENG yarn by applying PTFE and conductive polyamide as sheath and core yarn respectively, providing an acid and alkali-resistant ability for textile based on a core-sheath TENG yarn [70].

The third type is fabric-based NGs [71]. Xia et al. developed a fabric-based TENG based on nickel–copper bimetallic hydroxide nanowrinkles, named NC-TENG. Nickel-copper bimetallic hydroxide coated carbon cloth substrate was employed as a triboelectric layer and electrode. PTFE film was selected as another triboelectric layer and electrode. The output of the NC-TENG with size of 1 cm × 1 cm can reach 328 V and 36.15 μA. Maximum power density was 1.323 mW cm^{-2} [72]. T Though compared with yarn/fiber based TENG, the repetitive mechanical pulses always lead to the degradation of TENGs. However, fabric-based TENGs by coating different synthetic polymers on the surface are not breathable and not comfortable. Xiong et al. developed a durable skin-touch-actuated textile-based TENG. Black phosphorus encapsulated with hydrophobic nanoparticles was coated on PET fabric, which was employed as a synergetic triboelectric trapping layer and provided TENG with long-term durability under different conditions (500 cycles of fold, twist, stretch. 1150 rpm washing for 72 h). Based on single-electrode mode, the contact and separation between skin and fabric can lead to the electron flow and generate output. Under a 5 N, 4 Hz applied force by hand, the output reached 880 V and 1.1 μA cm^{-2}. Under slightly friction with skin, the TENG can generate outputs of 60 V and 9 nC cm^{-2} [73]. Qian et al. developed a TENG cloth. PDMS/3D bilayer graphene (BLGr) was selected as a negative triboelectric material and electrode, and Au/PET was employed as another triboelectric material and electrode. Compared with 2D BLGr, 3D BLGr had a larger contact area and better flexibility and structural stability. Under a vertical force of 6 N, 5 Hz, the output was 70 V, 9.3 mA cm^{-2}, and 0.65 mW cm^{-2}, respectively [74]. Zhu et al. developed a self-powered sock by coating poly(3,4-ethylenedioxythiophene) polystyrenesulfonate (PEDOT:PSS) on the cotton socks and integrated with lead zirconate titanate (PZT) piezoelectric chips (Fig. 3c). With PTFE film covered on the shoes, the contact and separation between socks and shoes can generate both triboelectricity and piezoelectricity. Under 2 Hz mild jumping and external load of 59.7 MΩ, an output power of 1.71 mW was collected. In addition, the sensor had a sensitivity of 0.06 V N^{-1}. The socks were used for walking pattern measurement, motion tracking, gait analysis and sweat detection [75].

3.2. Flexible film-based NG

Besides textile-based NGs, flexible nanogenerators are another energy harvest approach for wearable devices. Mounted to skin or cloths, the mechanical energy can be converted to electricity efficiently (Table 1).

Piezoelectric effect is based on the piezoelectric property of materials. Therefore, in order to develop flexible PENG, flexible piezoelectric materials should be selected, including piezoelectric ceramics like lead zirconate titanate (PZT), organic materials like PVDF, piezoelectric crystal such as zinc oxide (ZnO) nanowires [76]. Piezoelectric ceramics are fragile. To develop flexible PENG based on piezoelectric ceramics, a flexible substrate is needed. In 2013, Park et al. using laser lift-off (LLO), transferred thin PZT film to flexible polyethylene terephthalate (PET) substrate, developed a flexible piezoelectric PZT thin film nanogenerator. It showed an output performance of 200 V and 150 μA cm^{-2} [77]. Hwang et al. used solid-state single crystal growth (SSCG) method, growing a single crystalline piezoelectric $Pb(Mg_{1/3}Nb_{2/3})O_3$(PMN)–PZT thin film. Then the piezoelectric PMN-PZT thin film was adhered to flexible polyethylene terephthalate (PET) substrate, developing a flexible PMN-PZT PENG. The voltage and short-circuit current were 100 V and 20 μA [78]. In 2021, Huang et al. developed an anisotropic piezoelectric network composite(HAPNC) sensor based on Kirigami-structure. HAPNC was the core element of the sensor, consisted of a Kirigami-structured PZT network and PDMS matrix. The honeycomb piezoceramic Kirigami was proposed via a modified template-assisted sol-gel method, improved the piezoelectric properties and provided high-dimensional anisotropy to bending angles (17.3 times from 90° to 0°) for the sensor. PET flexible substrate and PDMS infiltration provided the flexibility and stretchability for the sensor. This sensor not only can measure the magnitude of stress, but also the stress direction. They further established a monitoring and alarm system for joint motion monitoring and prolonged sedentary behavior alarm [79]. Compared to inorganic piezoelectric materials, PVDF and its copolymer P(VDF-TrFE) itself has excellent flexibility and stretchability. In 2014, Pi et al. developed a flexible PENG based on P(VDF-TrFE) thin film by coating P (VDF-TrFE) thin film on the polyimide substrate. Depending on the direct piezoelectric effect, the output was 7 V, 58 nA, 0.56 μA cm^2 respectively [80]. Because the piezoelectricity of PVDF is not high, infill piezoelectric inorganic materials with flexible PVDF can improve the piezoelectricity as well as maintain excellent flexibility. Chen et al. proposed a high-performance PENG by embedding micropillar array of $BaTiO_3$ nano-particles into P(VDF-TrFE) polymer, which significantly enhanced the piezoelectricity [81]. In 2006, Wang et al. first developed PENG based on ZnO nanowires [42]. PENG based on ZnO nanowires has good piezoelectricity, but the flexibility is relatively poor. To develop flexible PENG based on ZnO, combined with flexible substrates is the most commonly used strategy. Deng et al. developed a flexible self-powered piezoelectric sensor (PES) based on cowpea-structured PVDF/ZnO nanofibers, which showed good flexibility and sensitivity (0.33 V kPa^{-1}, response time 16 ms. 4.4 mV deg^{-1}, response time 76 ms) [82].

Flexible materials and stretching structures are the two key points for the fabrication of flexible TENG. Traditional structure for flexible film-based TENG is sandwich structure. Some novel stretching structures like wavy structure and sponge structure also have been proposed [83]. Because triboelectric effect is a widespread phenomenon, there are a variety of flexible materials can be used for TENG fabrication. Flexible metal, [84]. flexible polymers, such as kapton, polyester, PDMS, silicone, which shows excellent durability, flexibility and high charge density, have been widely used in TENG fabrication [85]. Zhang et al. developed an ultrathin stretchable single-electrode TENG(CT-TENG). They employed thermoplastic polyurethane (TPU)-carbon black (CB) composite as stretchable electrode and triboelectrification layer. It was remarkably stretchable (≈646 %), ultrathin (≈50 μm) and lightweight (≈62 mg). Improved by postcharging treatment, CT-TENG can reach an output of 41 V [40]. Because of the Liu et al. developed a multi-mode stretchable and wearable triboelectric nanogenerator (msw-TENG) based on liquid metal and silicone for biomechanical energy harvesting. It showed an excellent stretchability and conductive characteristic. Under different applications, 3 working modes (contact separation/stretch/press mode) were transformed randomly [15]. Hydrogels, which have the properties of being self-healing, anti-freezing, low resistance increments with strain and biocompatibility, are ideal materials for TENG [86]. In 2017, Pu et al. proposed a soft skin-like TENG for energy harvesting and sensing. Ionic hydrogel (polyacrylamide (PAAm)) with lithium chloride (LiCl)) was selected as triboelectrification layer, and elastomer (PDMS or VHB) was the flexible electrode. It was extremely stretchable (uniaxial strain, 1160 %), transparent (96.2 % for visible light) and achieved a peak output of 35 mW m^{-2} [87].

Hybrid flexible nanogenerators can compensate the deficiencies of single working mechanism and maximum the energy conversion efficiency, which have attracted wide attention [88]. Inspired by shark gill, Zou et al. developed a stretchable bionic shark gill respiratory sensor (BSG-RS) based on tribo-piezo hybrid nanogenerator. It was fabricated by several parallel strip-shaped power generation units. Each of the unit was formed by a sandwich structure, which was silicone, PVDF piezo film and PDMS and PVDF. Based on the structure, BSG-RS can realize real-time respiration monitoring accurately and recognize different breathing pattern [89]. Because PVDF also has the pyroelectric property. Wang et al. developed a highly transparent and flexible hybrid nanogenerator based on triboelectric–piezoelectric–pyroelectric effect. PVDF was both triboelectric, piezoelectric and pyroelectric material. Thermal and mechanical energies can be converted into electric simultaneously, which showed a better performance than individual harvesting unit [90].

Table 1
Summary of Flexible-film based wearable NGs.

Working mechanism	Materials	Size	Output	Application	Ref.
single-electrode, contact-separation TENG	Elastomer (PDMS/VHB), PAAm-LiCl hydrogel	3 cm × 5 cm	145 V, 1.5 μA	electronic skin, tactile sensing	[87]
Single-electrode TENG	carbon black, TPU	2 cm × 4 cm	41 V, 0.262 μA	Breathing, pulse, pronunciation, joint motion monitoring	[40]
Contact-separation TENG	Silicone rubber, PDMS, Cu mesh	3 cm × 1 cm	2.52 V, 68.1 pA	Gesture recognition	[91]
PENG	$BaTiO_3$ P(VDF-TrFE)	1 cm × 1 cm	13.2 V, 0.33 μA cm^{-2}	Respiration sensing	[81]
PENG	PVDF, ZnO	N/A	0.33 V Kpa^{-1}	Gesture recognition	[82]
PENG	PET, AgNWs, ITO, PDMS, PZT composite	1.5 cm × 1.5 cm	945 mV	Joint monitoring	[79]
Piezo-Tribo NG	Silicone, Ag, PVDF	2.5 cm × 4 cm	45 V, 150 nA	Joints monitoring	[92]
Tribo-Piezo-Pyro NG	ITO, PVDF, PDMS	N/A	0.6 V, 20 μA	N/A	[90]

3.3. Integrated NGs

Apart from directly contact to the body, some NGs are integrated to common wearable equipment to meet the demand of IoTs. Jiang et al. developed a noncontact free-rotating hybrid nanogenerator (WRG) based on TENG and electromagnetic generator and integrated with shoes. Depending on a special mechanical transmission structure, the maximum rotating speed was 13.74 rps. Output can reach up to 14.86 mJ each step, which was much higher than traditional nanogenerators. A single external force stimulation can lead to a continuous output over 2 s. Integrated with shoes, the WRG can meet the power demand of most information electronics(1–5 V and 0.1–10 mA) like GPS [93]. Du et al. developed an insole hybrid nanogenerator based on TENG and PENG with a maximum output of 150 V and 4.5 μA. It had the abilities of distinguish different motion states and artery signals detection [17]. Mask is another common equipment integrated with nanogenerators. Airflow induced mechanical change can lead nanogenerator to generate electricity. Zhang et al. developed TENG-integrated mask for human-machine interaction, which based on single electrode mode. Nanowire structured polyethylene terephthalate (PET) thin film was employed as triboelectric layer. The TENG had a size of $0.5 \times 2 \times 3.5$ cm and weight of 2.47 g. Under normal respiration, output was 87 V and 0.4 μA respectively and 342 V and 2.3 μA under strengthened breath. The output difference can be utilized to distinguish the breath pattern and used for human-machine interaction [94]. Han et al. developed a triboelectric band, which was consisted of rubber tube filled with physiological saline. When contacted the skin, the rubber will be negatively charged. With the concentration and relaxation of muscle, the contact area change between the electrode(physical saline) and skin led to the potential difference, resulting in electrons flow. The peak output of the band was 89.4 V, 7.1 $\mu C\,m^{-2}$, and 0.62 $mA\,m^{-2}$. Maximum power density was 0.33 $mW\,m^{-2}$. Tied to the muscle, the band can distinguish different gait pattern for identification and authentication because muscle volume and gait is unique for each individual [95]. Luo et al. developed a bending-angle triboelectric nanogenerator(BA-TENG) and integrated with a glove for human-machine interface application. PDMS and silicone rubber were applied as the triboelectric materials [91].

4. Applications of NGs in orthopedics

The musculoskeletal system is one of the significant parts of the human body, which is closely related to the locomotion function. With the increase in life expectancy and the rapid increase in the elderly population, The incidence of both chronic and acute orthopedic diseases has greatly increased [96]. For example, it was reported that from 1990 to 2017, osteoarthritis have shown a 107 % increase in crude incidence rate, which will even continue to increase [97]. In the clinical orthopedic work, communication between patients and physicans is limited to diagnosis and treatment. But preclinical diagnosis and prevention as well as postclinical rehabilitation are also very important, early diagnosis, prevention and proper rehabilitation can minimize the harm. However, this procedure always lacks the participation of physicians. Therefore, making bridge between patients and physicans is critical in orthopedics. Because the unique working mechanism, not only can NGs work as an energy supply, but also provide real-time monitoring, especially for musculoskeletal system. In addition, the generated electricity also can be used for tissue stimulation. All of these advantages fit the demands of diagnosis, prevention and rehabilitation of orthopedic diseases and has a huge potential in orthopedic clinical work (Table 2).

4.1. Joint motion monitoring

Joint motion is critical in orthopedic diseases and sports medicine. Abnormal motion is generally related to the initiation and progression of most biomechanical orthopedic diseases. It can also predict the prognosis after surgery and the efficiency of rehabilitation. For example, osteoarthritis is a chronic joint disease with high incidence. It can affect almost all joint like hip, knee, and hand [98,99]. Range of motion (ROM) of joints is significantly correlated with the severity of osteoarthritis [100]. In daily activities, especially during exercise, joints are bent and stretched repeatedly. Excellent robustness and high stretchability are required for the sensors. Stretchable TENG or PENG can be used for ROM detection. By attaching to the joints, the variation of bending angle will lead to output change accordingly (Fig. 4a) [92,101]. However, the accuracy of those stretchable nanogenerators was not high, which can only satisfy the demand of healthy individuals. For patients, ROM is important to guide treatment. For example, exercise is vital for patients after orthopedic surgeries. In order to accelerate rehabilitation, doctors usually require patients do some specific exercise as early as possible after surgery, in which each specific exercise should achieve a specific ROM [102]. To develop the monitoring accuracy, Wang et al. developed a light and thick self-powered angle sensor (SPAS) based on TENG (Fig. 4b), which was integrated by two rotary contact-sliding TENG. It had a high resolution, sensitivity and signal-to-noise (SNR) ratio of 2.03 nano-radian, 5.16 V/0.01°, 98.68 dB respectively. Integrated with

Table 2
Summarize of the applications of wearable NGs in orthopedics.

Function	Wearable type	Mechanism	Materials	Performance	reference
Joint motion monitoring	Flexible film	PENG- Single electrode TENG	Silicone, Ag, PVDF	PENG mode:16 V, 175 nA TENG mode: 45 V, 150 nA	[92]
	Brace-integrated	Free-standing TENG	Kapton	Average $V_{oc:}$ 123.09 V 5.16 V $0.01^{\circ -1}$	[16]
Gait monitoring	Insole-integrated	Contact-Separation TENG	Rubber, Cu, PET	35 V, 0.25 μA	[108]
	Insole-integrated	PENG array	PVDF	0.016 V Kpa^{-1}	[119]
	Socks-Insole integrated	Contact-Separation TENG	Chitosan-glycerol film, PTFE	130 V, 10 mA m^{-2}	[120]
Muscle Function Monitoring	Flexible film	Contact-Separation TENG	Parylene-C, Silicone, PVA, PEI, LiCl	78.44 V, 1.42 μA	[127]
Rehabilitation	Flexible film	Contact-separation TENG-driven microneedle	PET, Ag, PVDF, Cu, Kapton	1 V, 2 μA	[19]
	Textile	Contact-separation TENG	Conductive textile, Nitrile, Silicone Rubber	5 V, 13 μA	[137]
Cardiovascular monitoring	Textile	Contact-Separation TENG	CNTs, FEP, Al, PDMS	0.21 μA Kpa^{-1}	[150]
Respiration monitoring	Mask-integrated	PyNG	PVDF, Al	42 V, 2.5 μA	[159]
Temperature monitoring	Flexible film	Contact-Separation TENG	Paper, MoS_2 glue, Graphite Glue	3.82 V, 0.20 μA	[171]

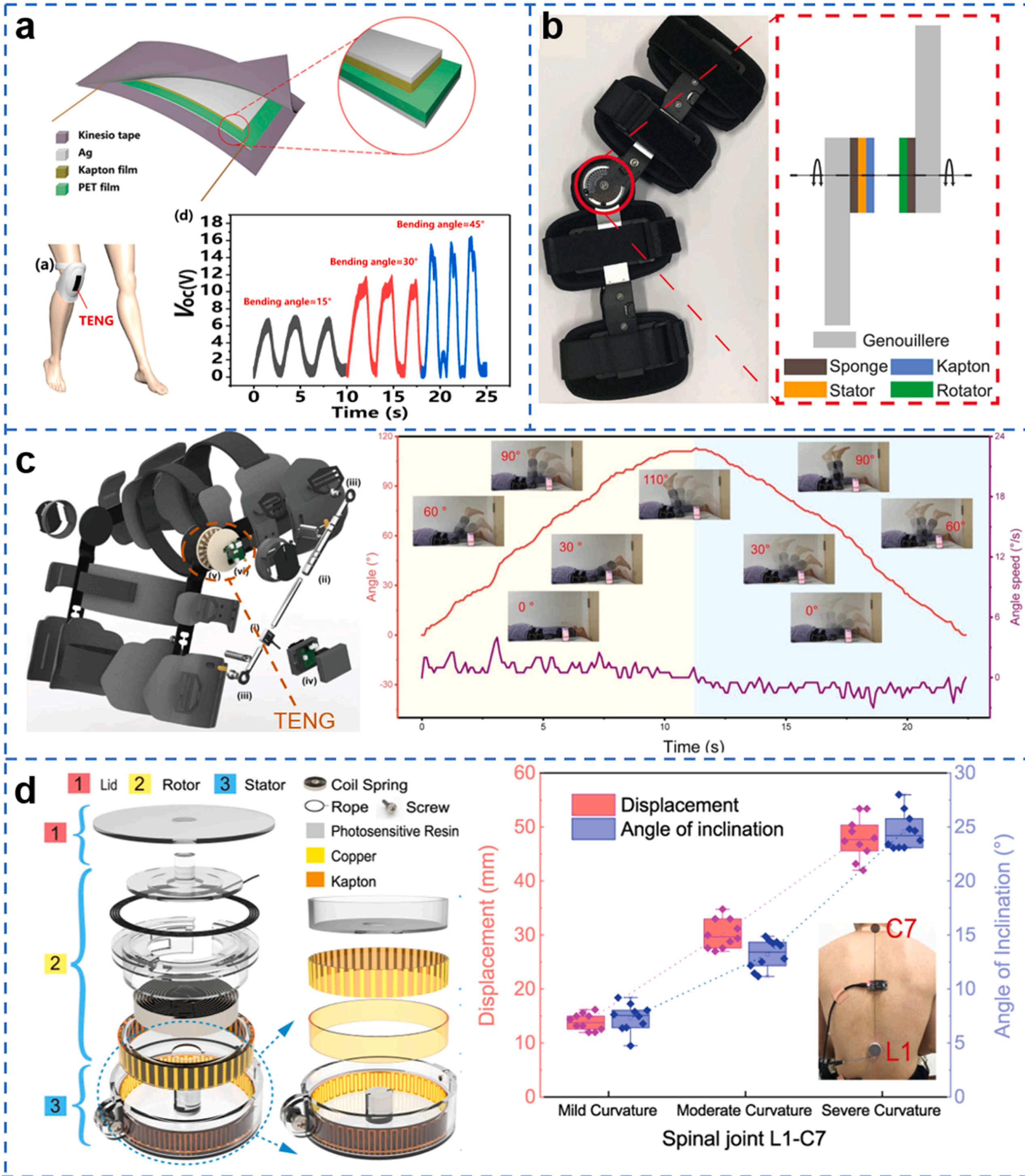

Fig. 4. (a) Strain sensor based on TENG for joint bending angle detection [101]. (b) Self-powered angle sensor (SPAS) based on two rotary contact-sliding TENG for joint angle detection. Reproduced with permission [16]. Copyright 2020, WILEY-VCH Verlag GmbH & Co. KGaA, Weinheim. (c) Brace-integrated TENG for post-surgery rehabilitation [103]. (d) Grating-structured TENG for joint/spinal bending sensing [41].

brace, a dynamic measurement range achieved from 20° to 150° s^{-1}, which showed its potential application in orthopedics [16]. To assist post-surgical rehabilitation, Luo et al. developed an isometric myodynamia and rotation sensing system with high force and angle resolution by integrating TENG and wearable brace (Fig. 4c). Muscle force was measured by telescopic rods and characterized via a standard torque assessment platform. The force and angle resolution were 0.01 N and 1° respectively. Standard rehabilitation exercises are required for every patient for strength and ROM recovery. Briefly, certain angles of joint extension and flexion should be performed every day after surgery. But without the guidance of doctors, rehabilitation exercises are always not in place due to the lack of ROM measurement method. In order to verify the effect of TENG in post-surgery rehabilitation. They performed a clinical trial by comparing healthy people ($n = 10$) with patients who took total knee arthroplasty ($n = 14$). A notable rehabilitation enhancement was shown in patients using the device, which showed the attractive potential for smart care in post-surgery rehabilitation [103]. In many spinal diseases, the choice of operational technique is determined by the angle of deformities [104,105]. Li et al. developed a stretch sensing device based on grating-structured TENG for joint/spinal bending sensing (Fig. 4d). It was an integration of retractable badge reel and the grating-structured TENG, which was small and light: 33 mm in diameter, 10 mm in thickness, and 9.6 g in weight. The sensitivity (8 mm V^{-1}), resolution (minimal 0.6 mm), and durability (over 120 K cycles) were both excellent. With the bending or stretching of joints, the device can stretch or contract at the same time and the displacement

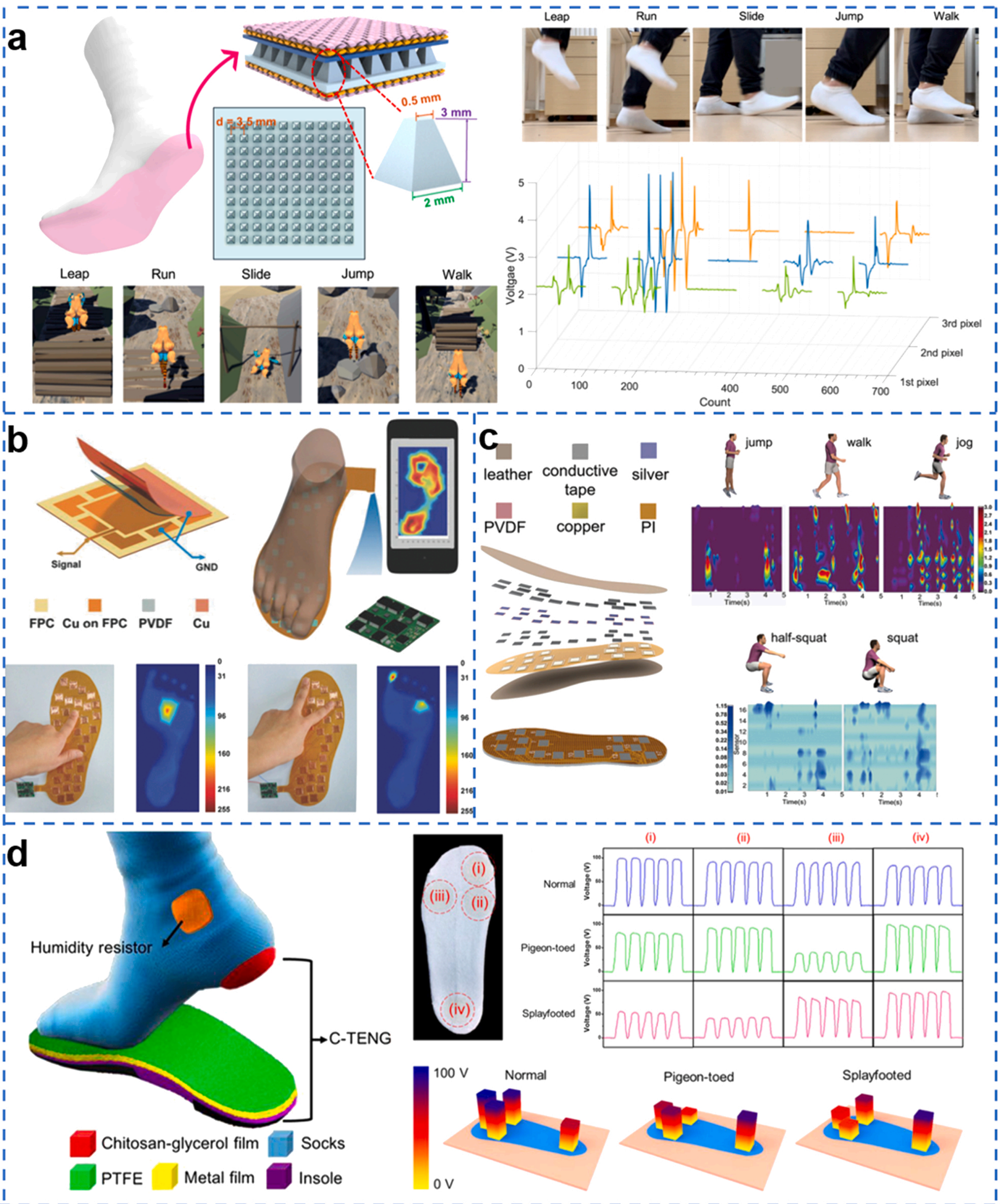

Fig. 5. (a) Deep-learning based TENG sock for gait analysis and VR application [111]. (b) plantar pressure mapping system based on PENG and EMG. Reproduced with permission [118]. Copyright 2018, WILEY-VCH Verlag GmbH & Co. KGaA, Weinheim. (c) PENG matrix array with machine-learning for LDD diagnosis and postoperative assessment. Reproduced with permission [119]. Copyright 2022, Wiley-VCH GmbH. (d) TENG textile for plantar pressure assessment. Reproduced with permission [120]. Copyright 2018, Elsevier Ltd.

change of the freestanding electrode will generate the voltage signals with different velocities. Recorded by monitoring terminal, the total displacement can be measured and to calculate the joint motion. By attaching to the spine, the device can also detect the spinal shape change. Because of its high linearity, it can sense joint motions precisely and accurately [41].

4.2. Gait monitoring

For the elderly, gait changes are generally physiologic, including walking speed reduction, postural changes, and balance deterioration. It will induce functional decline and impair quality of life [106]. There are various diseases that can also lead to gait changes, such as neuromuscular weakness, parkinsonism and ataxia [107]. Lin et al. proposed a gait monitoring insole based on TENG. It can distinguish different gait patterns and detect abnormal gait for rehabilitation assessment. They also proposed a fall-down alert system for warning of falling down. When the elderly or patients fall down, the insole can send an alert at once [108]. Gait retraining is an important non-surgical treatment for most lower limb diseases and an essential habilitation method [109]. Virtual reality (VR) shows its excellent performance in gait retraining [110]. Zhang et al. developed deep learning-enabled smart socks based on TENGs (Fig. 5a). For gait detection, a sensing range up to 200 kPa is needed, which is higher than the sensing range of traditional narrow-gap textile-based TENG. To improve the sensing sensitivity and range, they employed a silicon rubber with mm-scale frustum structure as one of triboelectric layer and Nitrile as another. The first linear range of a 3 cm × 3 cm TENG without frustum structure was 10–70 kPa, while the sensing range of TENG with frustum structure was extended to> 200 kPa. The extend of sensing range enabled the application in gait detection. Harvesting from normal walking, a sock can charge up a 27 μF capacitor in 3–4 min, which was enough to power a Bluetooth module and detect body temperature by embedded temperature sensor. Based on an optimized deep learning model, the socks reached an identification accuracy of 93.54 % and different activities detection accuracy of 96.67 %. They mapped the collected physical signals in the VR fitness game and shows the potential application in gait retraining [111]. Plantar pressure distribution is another important part of gait. It can reflect the joint moment to some extent [112]. Abnormal plantar pressure distribution indicates many diseases associated with foot. Study shows that there are significant foot pressure differences between the normal, planus and cavus foot [113]. For patients with abnormal foot postures, they are always not aware of their abnormality at the early stage, which makes them diagnosed and managed too late and impact on the ankle even the knee and hip [114]. Plantar pressure distribution abnormal also occurs in some hip and knee disorders like knee valgus/varus deformities and hip or knee osteoarthritis [115]. Plantar pressure distribution measurement based on the piezoelectric effect has been widely studied. several piezoelectric sensors are placed at the different sites of shoes, the distribution of plantar pressure can be output as electric signals [116,117]. Deng et al. developed a plantar pressure mapping system based on the integration of PENG, TENG and electromagnetic generator (EMG) (Fig. 5b). PVDF is employed as PENG pressure sensors. Driven by a hybridized triboelectric–electromagnetic nanogenerator, data can be collected and transmitted to mobile terminals by Bluetooth technology to realize real-time plantar pressure monitoring [118]. To improve the low spatial resolution because of few sensors and avoid insufficient formalistic parameters evaluation. Liu et al. developed a flexible insole with more than 30 piezoelectric sensing spots based on PVDF for plantar pressure monitoring (Fig. 5c). It showed a stability under 10,000 press cycles with 300 kPa. An AI recognition based on support vector machine supervised learning algorithm was employed for signals assessment, which showed an accuracy of 99.2 % in human motion recognition. Lumbar degenerative disease (LDD) is a common disease involves lumbar nerve, always leading to low back pain. The diagnosis of LDD in clinic is based on imaging examinations. Plantar pressure distribution has a relationship with LDD. They employed 62 LDD patients and 63 normal people to evaluate the predict accuracy in LDD diagnosis by AI. A 100 % diagnostic accuracy was shown in LDD recognition. Furthermore, excellent post-surgery recovery assessments were given out, which was corresponded well with doctor's suggestions [119]. Pressure distribution assessment based on TENG has also been developed. Jao et al. developed a chitosan-based TENG textile for multifunctional sensing (Fig. 5d). They coated chitosan-glycerol film on the different sites of socks and fabricated an insole by PTFE, the contact-separation of chitosan and PTFE resulting in the triboelectric output. Compared with traditional TENG, it showed a high stability under humidity condition. By coating chitosan at the different sites of socks, the TENG can detect force distribution of feet [120].

4.3. Muscle function monitoring

Skeletal muscle is the biggest tissue of body, which comprises about 40 % weight of body. Muscle function is closely related to nutrition status in physiologic [121]. In muscle diseases, like muscle atrophy, sarcopenia and muscle weakness, muscle assessment is essential for clinical guidance. Muscle strength, tone, mass are basic events for muscle assessment, in which muscle strength is the most essential measurement. Muscle activities are performed by the contract and diastolic of muscle fiber, generating muscle strength. In elderly, lower-limb strength is associated with static posture and dynamic postural compensation [122]. Isokinetic dynamometer is often used clinically to measure muscle strength. The resistance of the dynamometer is equal to the muscle strength when the motion. This method can be provided for a dynamic muscle strength measurement. In addition, it can apply optimal loading to muscles for rehabilitation, training and injury prevention [123]. However, this machine is unable to monitor muscle strength daily because it is too huge and should be operated by professionals. Strain sensors are promising in strength detection due to their resistance will change according to the change of strain. However, strain sensors need external power to drive [124]. Self-powered strain sensors can provide an intuitive muscle strength evaluation by the change of output current or voltage [125]. Because muscle activities are based on the contraction and relaxation of different muscle groups. Single muscle monitoring is unable to reflect muscle function in general. Chen et al. developed a stretchable and skin-friendly TENG with a structure of a double layer of silicone rubber (DS-TENG) embedded with Ni foam and Ag nanowire for 3D muscle sensing (Fig. 6a). By fixing 3 arranged DS-TENG around the muscle, tiny muscle motion can be detected [126]. Traditional TENGs have several limitations to constrain their application in the biological system, two of which are mechanical mismatch with tissues and metal electrode fragility under repeated deformation. By replacing metal electrode layer with ionic hydrogel, Wang et al. fabricated a stretchable and self-healing ionic hydrogel-based self-powered muscle function sensor based on TENG (Fig. 6b). The ionic hydrogel was developed by poly(vinyl alcohol) (PVA), polyethylenimine (PEI) and LiCl. The hydrogel showed excellent abilities of deformation tolerance and fast self-healing. Silicone rubber and parylene-C were employed as friction layers. Dielectric elastomer (VHB) and parylene-C were selected as the substrate and packaging layers, which can mount on skin and detect muscle directly. It showed a maximum output of 78.44 V, 1.42 μA, and 47.48 nC respectively. The output signals linearly corresponded to the applied force and angle, realizing direct and quantitative monitoring. Furthermore, it achieved a fast response time of 1.03 ms and low detection threshold of 0.2 mN and long durability up to 10^5 tests without performance degradation [127].

4.4. Rehabilitation

The symptoms of most orthopedic diseases are localized around the tissue, such as the pain and swelling from fracture and sprain. Chronic diseases like osteoarthritis, has the major symptoms of joint pain.

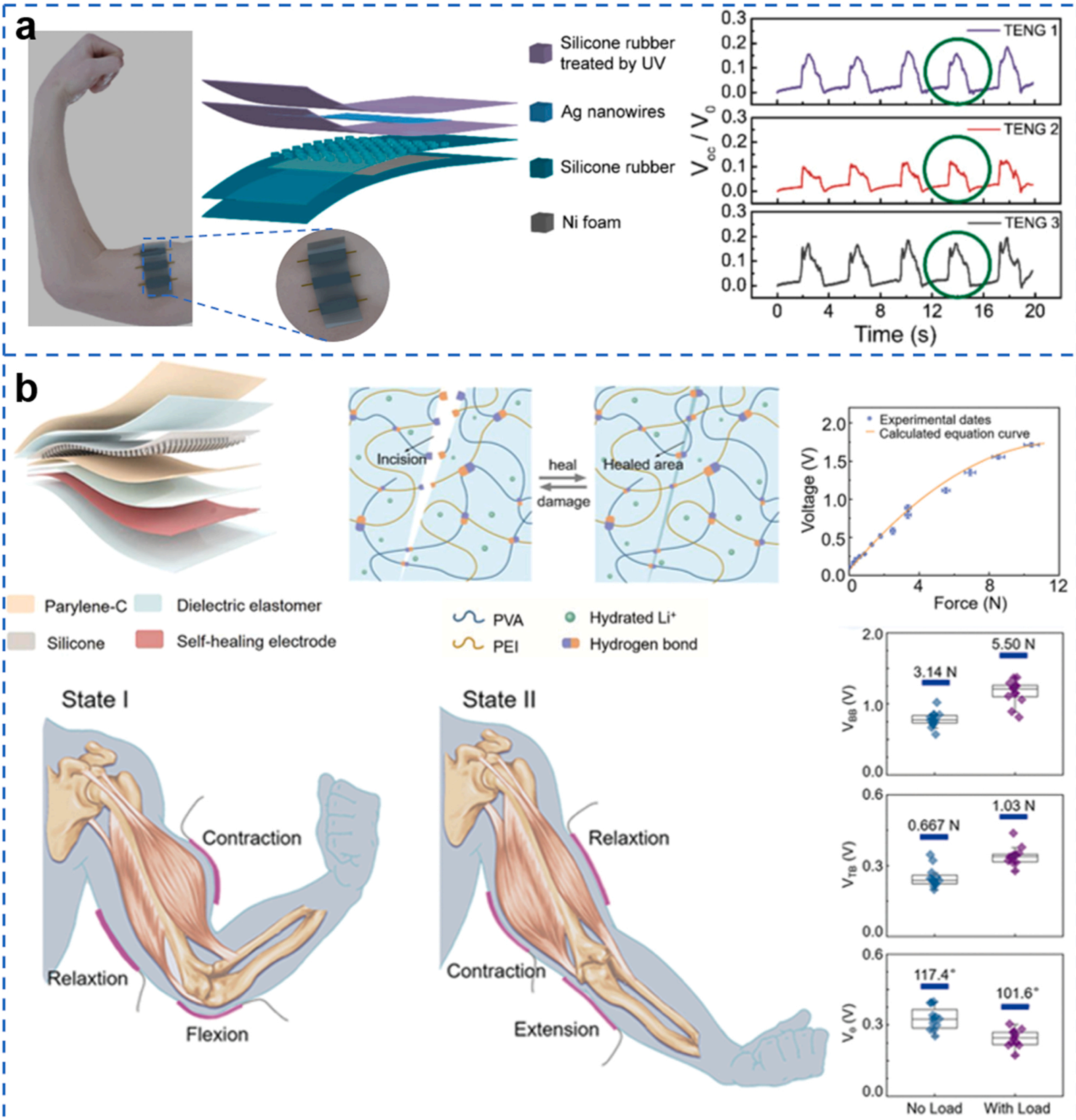

Fig. 6. (a) 3D muscle monitoring based on TENG. Reproduced with permission [126]. Copyright 2019, American Chemical Society. (b) Stretchable, self-healing, and skin-mounted active sensor based on TENG for muscle function assessment. Reproduced with permission [127]. Copyright 2021, American Chemical Society.

Nonsteroidal anti-inflammatory drugs (NSAIDs) like ibuprofen are recommended to relieve pain and anti-inflammation [128]. However, traditional drug delivery methods have several limitations. Oral drug delivery may induce liver or renal injury [129,130] and gastrointestinal damage [131]. Topical drug administration will not meet expectations due to the inability to penetrate the skin. Electricity is one of the commonly used strategies to improve penetration efficiency. Ouyang et al. developed a self-powered transdermal drug delivery system driven by TENG. The energy harvest from biomechanical energy was able to be stored in the power management circuit for adjust and stabilize, which was used to enhance the drug delivery efficiency. They successfully achieved tunable transdermal drug delivery from 0.05 to 0.25 μg cm^{-2} by changing TENG charging time or resistance of the power management circuit (Fig. 7a) [132]. Wu et al. developed an Iontophoretic drug delivery system for motion detection and therapy based on TENG (Fig. 7b). Hydrogel drug patch was electrically connected to the TENG. Driven by TENG, long-term drug delivery can be realized [133]. Simply using electricity to release drugs cannot achieve optimum delivery efficiency. Yang et al. developed a controllable transdermal drug delivery system (sc-TDDS) based on PENG and microneedles (MNs) array. PVDF was selected as the piezoelectric layer. For the fabrication of MNs, polylactic acid-gold-polypyrrole (PLA-Au-PPy) MNs array deposited with drugs was employed as working electrode (WE) as well as polylactic acid-gold (PLA-Au) MNs array as the counter electrode (CE). Under a certain voltage, drug can be released from WE. The voltage, current and transferred charge of PENG were 100 V, 2 μA and 300 nC respectively under linear motor and 50 V, 1 μA, 100 nC under gentle slap. They loaded dexamethasone in the NWs to treat psoriasis. Applied 1.5 V and 2

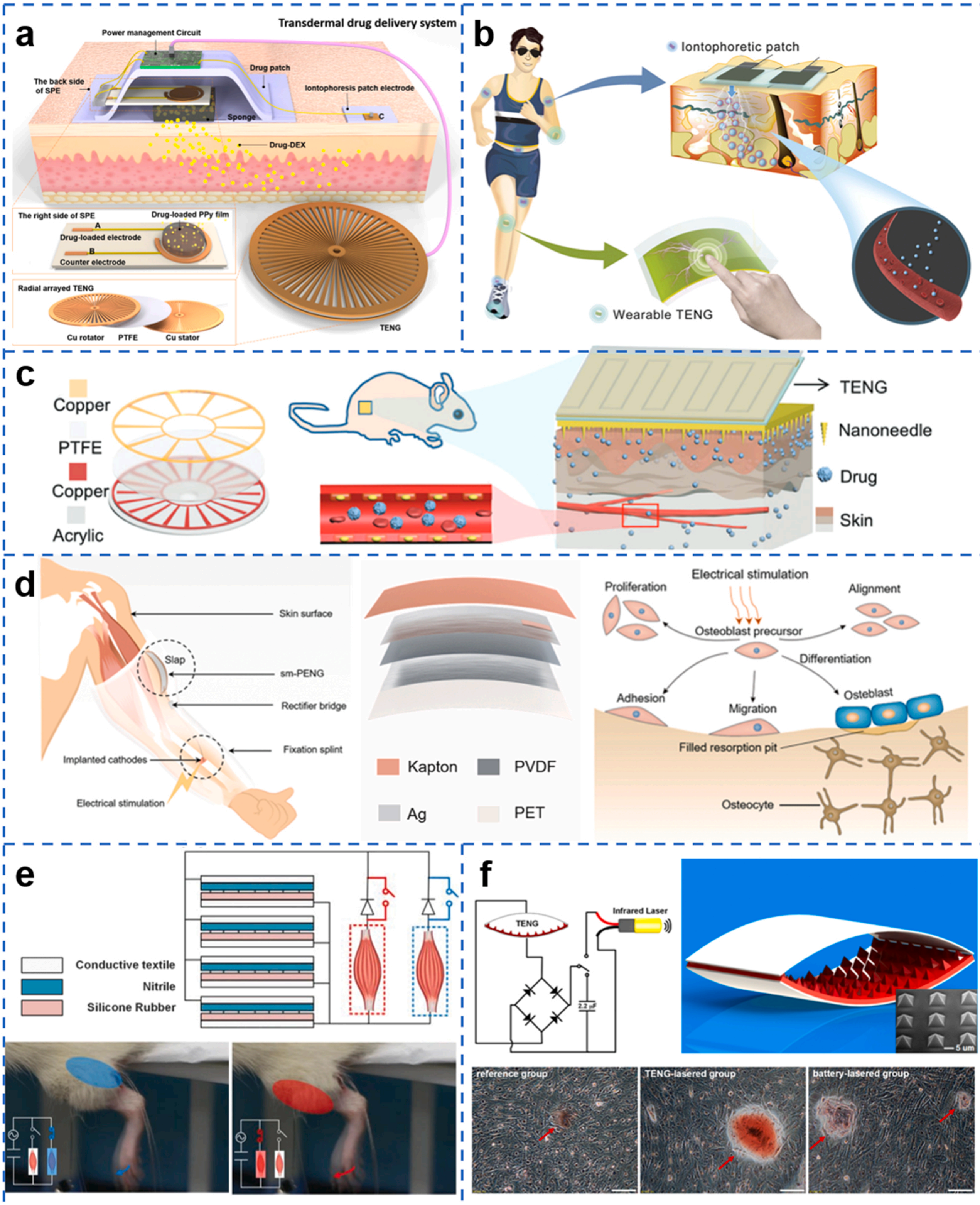

Fig. 7. Wearable nanogenerators for orthopedics rehabilitation. (a) On-demand drug release system based on TENG. Reproduced with permission [132]. Copyright 2020 Elsevier Ltd. (b) Iontophoretic Transdermal Drug Delivery System based on TENG. Reproduced with permission [133]. Copyright 2019, WILEY-VCH Verlag GmbH & Co. KGaA, Weinheim. (c) TENG-driven electroporation system for intracellular drug delivery. Reproduced with permission [134]. Copyright 2019 WILEY-VCH Verlag GmbH & Co. KGaA, Weinheim (d) Fixation splint with biomechanical-energy-driven shape memory piezoelectric nanogenerator(sm-PENG) to promote bone repair. Reproduced with permission [136]. Copyright 2021 Elsevier Ltd. (e) Direct muscle stimulation based on TENG [137]. (f) Self-powered low-level laser cure (SPLC) system for osteogenesis. Reproduced with permission [139]. Copyright 2015, American Chemical Society.

μA pulse electricity, the sc-TDDS can release 8.5 ng dexamethasone each stimulation and showed a promising effect on psoriasis [19]. Liu et al. developed a TENG-driven electroporation system for intracellular drug delivery (Fig. 7c). The system was structured by 4 components: a disk TENG as power source, rectifier bridge, a 5×5 mm silicon nanoneedle-array electrode as anode and aluminum (Al) electrode as cathode. The TENG was based on freestanding mode. Radially arrayed copper strips were selected as the rotator and one of the friction layers, and PTFE was selected as another friction layer for the disk TENG. Cranking in 1 s by hand, output frequency, output voltage, current and transferred charge was 20 Hz, 20 V, 4 μA, and 0.06 μC respectively, which could fulfill the demand of electroporation. The pulsed electric field was generated between anode and cathode by TENG will pass through nanoneedles to cells, resulting in electroporation. Traditional electroporation is always accompanied with the deficiencies of high voltage and its induced heat, causing low cell viability. They used silicon nanoneedle to enhance localized field at the nanoneedle-cell interface, thus reduced exerted external electric field and corresponding cell damage. Attached to the skin of mice skin, electroporation system can successfully deliver to a depth of 23 μm subcutaneous. Deeper than flat TENG (11 μm) and without electrical pulse (6 μm) [134]. In motor disorders, physiotherapies are critical because of the direct tissue stimulation [135]. Apart from drug delivery, nanogenerators have shown its promising applications in tissue electric stimulation. Zhang et al. integrated a fixation splint with biomechanical-energy-driven shape memory piezoelectric nanogenerator (sm-PENG) to promote bone repair (Fig. 7d). They formed an arched structure for sm-PENG by heating the Kapton film. Compared with short-circuit current of the flat structure (8.2 μA), arched structure was 20 μA by tapping. Direct electrical signal was generated after rectification. MC3T3-E1 cells showed an enhancement of proliferation, differentiation and acceleration of osteogenesis with no obvious side effect under the stimulation of 3 Hz, 20 μA, two hours per day, which showed a potential for bone repair application [136]. To further investigate how the triboelectric stimulation affects bone repair, Wang et al. developed a wearable pulsed TENG (WP-TENG). A peak output of 30 μA successfully rejuvent aged bone marrow mesenchymal stem cells (BMSCs) and promoted osteogenic differentiation and angiogenesis via mechanosensitive ion channel Piezo1 activation, which provided a theoretical basis for the applications of TENG in bone regeneration [18]. Electric stimulation also have displayed the potential in muscle repair. He et al. integrated a narrow-gap TENG textile with a high-voltage diode (D-T-TENG) and a textile-based switch to enhance the output of TENG (Fig. 7e). The closed-loop current of D-T-TENG (about 13 μA)) was higher than bare textile TENG (about 0.5 μA) at the same condition. They used D-T-TENG to direct stimulate muscle and sciatic nerve, both founded a force recovery [137]. To investigate the advantages of muscle stimulation by TENG compared to conventional methods. Wang et al. developed a stacked-layer TENG and a multiple-channel epimysial electrode for direct muscle stimulation. They found that the low-current of TENG with systematic mapping electrode can achieve an optimum stimulation efficiency. Moreover, long duration waveform generated by TENG was more stable than square wave and enveloped high frequency wave. Long pulse duration and low current can reduce the side effect of muscle stimulation and provided a theoretical basis for muscle stimulation by TENG [138]. Except direct electrical stimulation, other physical stimulations are also attractive. Tang et al. developed a self-powered low-level laser cure (SPLC) system for osteogenesis (Fig. 7f). They fabricated a flexible TENG by employing PDMS and indium tin oxide (ITO) as the friction materials. Infrared laser was driven by TENG trigger by linear motor with a frequency of 50 Hz and displacement of ± 0.5 mm (100 pulses/day). The wavelength, irradiation diameter and power of infrared lased was 850 nm, 6 mm and 10 mW respectively, which means the power density was about 35.4 mW m^{-2}. MC3T3-E1 proliferation and differentiation enhanced significantly after the infrared laser treatment [139]. Thermal therapy based on TENG also has been proposed. Yang et al. designed a self-healing and elastic single-electrode TENG based on poly(dopamine) (PDA)-CNT/PVA hydrogel encapsulated with self-healing silicone elastomer. Due to the photothermal effect of PDA-CNT, under a 5 min near-infrared laser irradiation, the temperature of TENG can gradually increase from 25 to 60 °C, which was able to be used for joint thermal therapy [20].

4.5. In vital signals monitoring

The human body is composed of multiple systems that work together in coordination to maintain life activities Typically, in the clinical practice of orthopedics, adequate assessments of each patient are essential to provide guidance for preoperative intervention, treatment selection, postoperative care and rehabilitation. Cardiovascular monitoring, mainly including rhythm, heart rate, blood pressure, and electrocardiogram (ECG), is to identify high-risk patients with underlying cardiovascular diseases [140]. Respiration monitoring consists of breathing rhythm, rate and exhaled gas that is constituent to assess postoperative pulmonary complications [141]. Meanwhile, body temperature monitoring is an important indicator of infection [142].

4.5.1. Cardiovascular monitoring

With the life expectancy increasing significantly and globally, the incidence of chronic diseases is increasing substantially, especially in low-income and middle-income countries. Among them, cardiovascular diseases account for a major part. Early diagnosis and prevention can decrease the health burden and cost [143,144]. In orthopedics practice, especially pre- and post-surgery, cardiovascular assessment is required [145]. The most common principle of TENG/PENG-based wearable cardiovascular monitoring devices that subtle skin vibrations caused by arterial pulse can be converted into electricity (Fig. 8a) [15,146–148]. To further improve the detecting sensitivity. Xu et al. demonstrated a d a self-powered ultrasensitive pulse sensor (SUPS). They employed polyamide (PA) thin films and Fluorinated ethylene propylene (FEP) as triboelectric layers due to the optimal electrical output. The SUPS showed the ultrasensitivity of 10.29 nA kPa^{-1} under low pressure condition. They proposed a new method for cardiovascular monitoring via SUPS. By placing at the different arteries to detect pulse waveforms and extracting peak position difference, most of indicators of cardiovascular system can be precisely predicted, including heart rate, pulse wave velocity, and blood pressure, which was highly concordant with commercial medical devices (Fig. 8b) [149]. Based on the detected pulse signals through single device, some researchers transmitted them into blood pressure signals through machine-learning. Fang et al. developed a machine-learning enhanced textile pulse sensor based on TENG. The structures of the sensor including: i) External textile to protect against airflow noise and repel moisture. ii) single-walled CNT cotton film as one of the triboelectric layers as well as lead-out electrode. iii) nonwoven FEP textile with highly negative electron affinity as another triboelectric layer. iv) PDMS as the biocompatible and waterproof material. It was light-weight (0.27 g) and thin (225 μm). Good performance was shown, with a signal-to-noise ratio of 23.3 dB, response time of 4 ms, and sensitivity of 0.21 μA kPa^{-1}. After machine-learning, the systolic and diastolic blood pressure only had relatively small mean deviations of 2.9 % and 1.2 % compared with commercial blood pressure cuff [150]. Microstructures have been proven can increase the sensitivity of PENG [151]. Tan et al. introduced a microstructure of PLA columnar array to develop a blood pressure monitor wrist band based on PENG. PVDF was selected as the piezoelectric material. A higher signal-to-noise ratio of about 29.7 dB was achieved. The peak output of sensor was 0.41 V, 0.21 μA and 45 nC. Based on the transformer deep learning model, the sensor can predict pressure with the error less than 4 mmHg (Fig. 8c) [152].

4.5.2. Respiration monitoring

Respiration is critical but has always been considered not directly

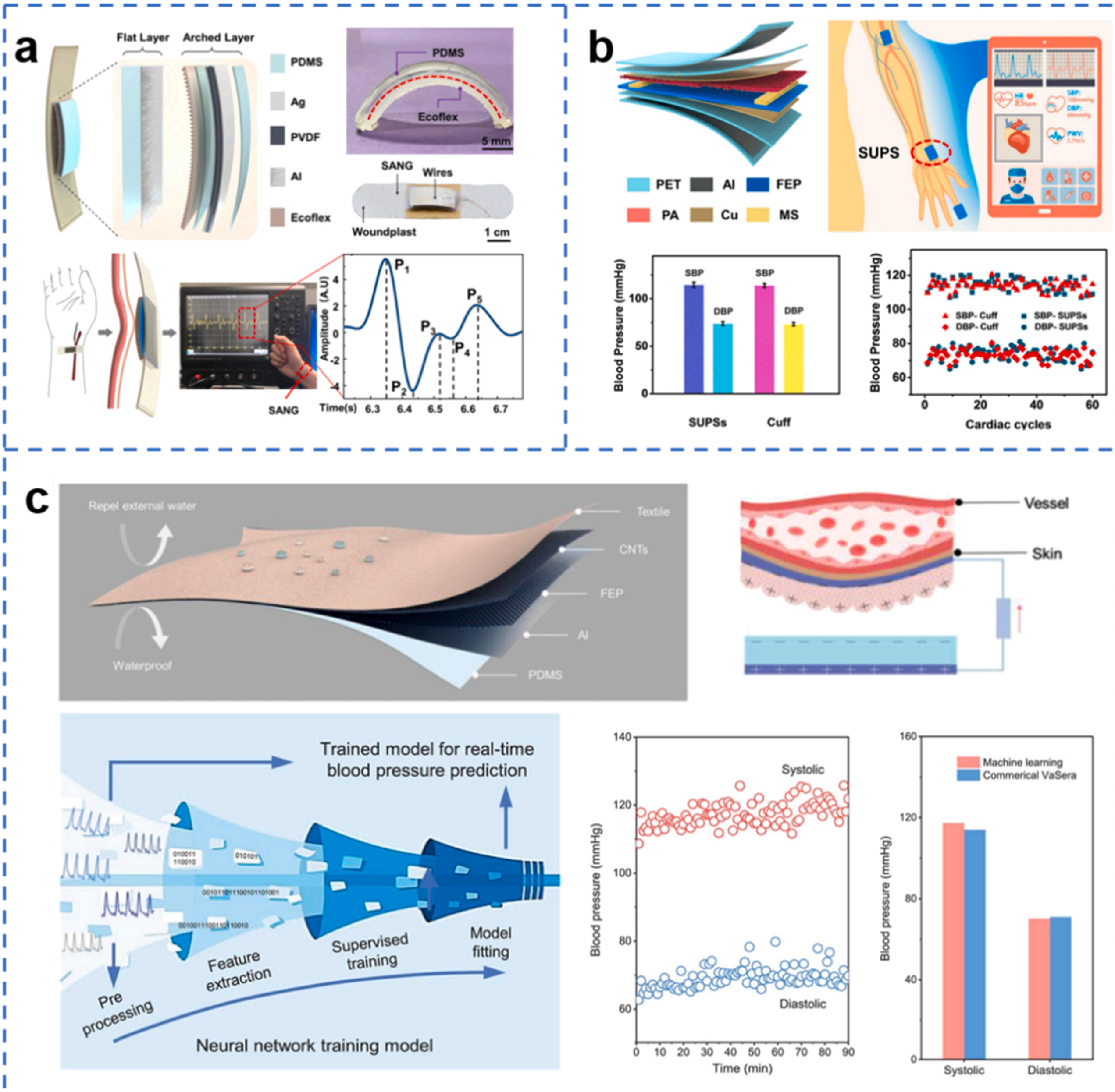

Fig. 8. Nanogenerators for cardiovascular monitoring. (a) A self-arched hybrid nanogenerator for pulse detection. Reprinted with permission [148]. Copyright 2020, Elsevier Ltd. (b) self-powered ultrasensitive pulse sensor (SUPS) for cardiovascular monitoring and blood pressure measurement. Reproduced with permission [149]. Copyright 2020 Elsevier Ltd. (c) Machine-Learning-Assisted Textile TENG for cardiovascular monitoring. Reproduced with permission [150]. Copyright 2021 Wiley-VCH GmbH.

correlated in orthopedics. In clinic, common degenerative musculoskeletal diseases often lead to the decline of respirational functions [153,154]. Especially while under anesthesia or postoperative pain, pulmonary function change will further lead to gas exchange impair and functional decline [155]. Perioperative respirational monitoring effectively prevents pulmonary complications due to underlying diseases and surgical stress response [156]. Respiration rate and rhythm are easy to detect by TENG and PENG. With the breath induced regular chest deformation or airflow-driven mechanical vibration, respirational patterns can be detected by the change of electrical signals [157,158]. Considering the temperature of human body is about 37 °C constantly, there will always be an evident temperature difference between exhaled gas and environment, extremely in winter. Xue et al. developed a wearable breathing sensor based on PyNG to utilized this temperature difference for respiration and temperature monitoring. A 3.5 cm × 3.5 cm PVDF film was selected as the pyroelectric material and attached to a common N95 mask. Under 5 °C ambient temperature, the output of PyNG was 42 V, 2.5 μA respectively. Maximum power was 8.31 μW with 50 MΩ external load. The circuit output indicated rhythm and rate of respiration. In addition, the output signals were linearly dependent on the ambient temperature, which can be applied for temperature monitoring (Fig. 9a) [159] Due to the mechanical energy of airflow, TENG also can used for respirational monitoring. Wang et al. developed a nanostructured PTFE (n-PTFE). By placing in an acrylic tube, airflow-driven vibration can generate real-time electric signals, which can be used for respirational monitoring [14]. In clinic practice, strategies for patients with chronic diseases must be adjusted in order to avoid the side effect of conventional treatments. In addition, chronic diseases should be treated or controlled before surgery. Thus, blood examinations are routinely taken in order to check systematic body

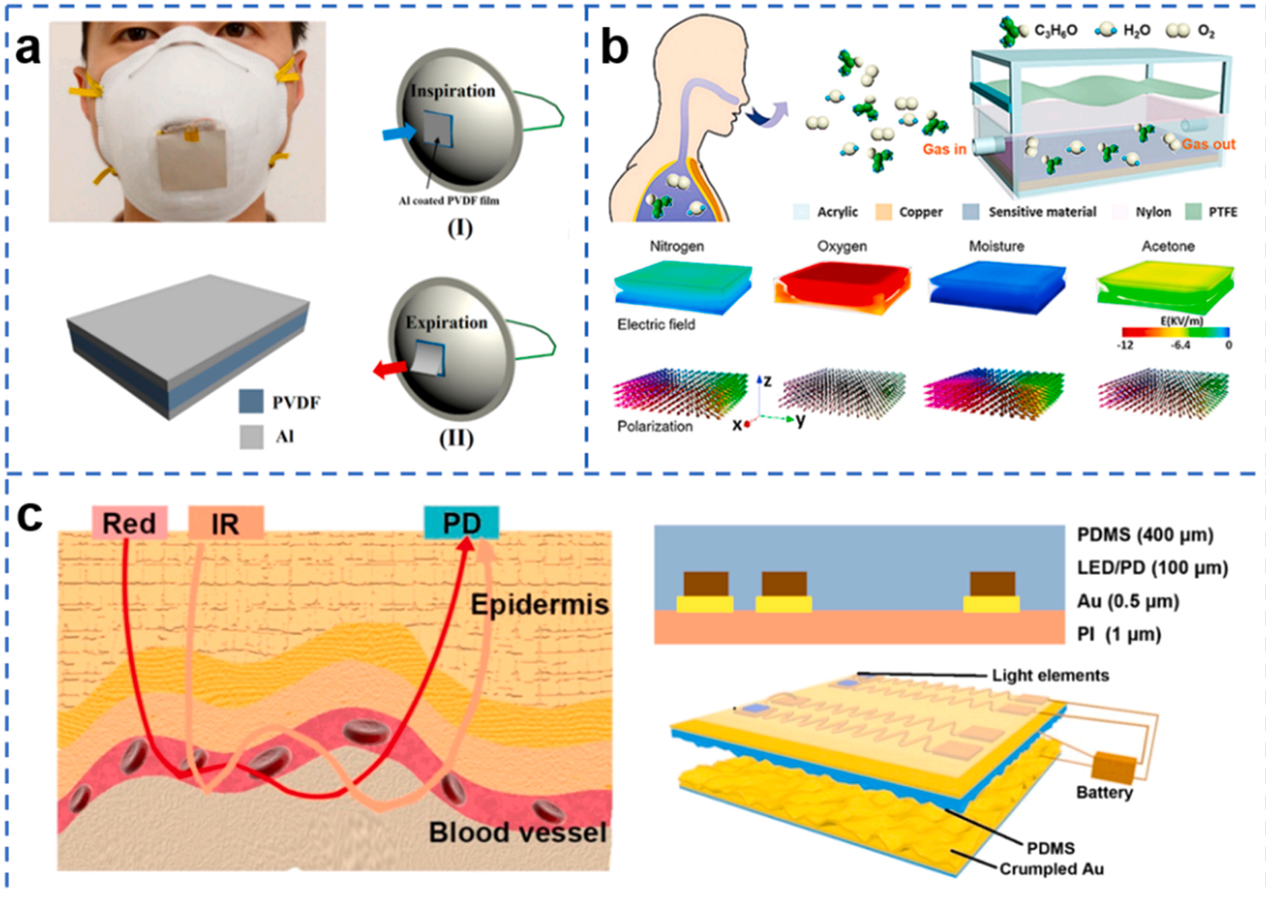

Fig. 9. Self-powered wearable devices for respirational monitoring. (a) Self-powered mask based on PyNG for respiration and temperature monitoring [159]. (b) TENG for respiration acetone detection. Reproduced with permission [163]. Copyright 2020 Elsevier Ltd. (c) TENG for blood oxygen detection [165].

condition. But blood examinations are invasive and painful. Respirational chemical reagents examinations now are as substitute for some diseases' diagnosis. However, some patients need long-term monitoring. Though commercial wearable respirational monitoring devices can provide at-home monitoring, frequent charging and bulk size limited patients daily activities to some extent. Some vital respiratory chemical reagents detection based on nanogenerators has been developed [160]. Acetone is one of the products of metabolism. Respirational acetone level is associated with blood sugar level and diabetic mellitus [161, 162]. By coupling triboelectric effect and chemisorption, Su et al. developed a self-powered acetone sensor for respiration monitoring and prediabetes diagnosis (Fig. 9b). PTFE and nylon film were selected as the triboelectric layers, chitosan and graphene oxide (rGO) were employed as sensitive materials. Driven by the air flow, periodic contact and separation between two triboelectric layers will lead to the electric output. Generated electricity was transmitted wirelessly to the gas interface for acetone detection. Under 10 ppm acetone, a sensing response of 70.36 % was reported [163]. Lung diseases like chronic obstructive pulmonary disease (COPD), tuberculosis (TB), and lung carcinoma need a long-term blood oxygen monitoring, which is vital to indicate pulmonary ventilation function and gas exchange [164]. Chen et al. developed a self-powered sensor for blood oxygen and pulse rate monitoring based on TENG [165]. The TENG was stretchable and flexible based on PDMS triboelectric layer and crumpled Au electrode. Voltage, current, and power density was 75.3 V, 7.4 μA, and 0.2 mW cm^{-2} respectively. Blood oxygen detection was realized by photoplethysmography (PPG). PPG is an optical technology to detect the change of blood volume on the surface of skin. Briefly, hemoglobin with different oxygen level show different colors. Light from LED after penetration and reflection through epidermis can be detected by PPG, which reflects the blood oxygen level [166]. By combining TENG and PPG, the sensor showed the potential to monitor pulse and blood oxygen real time (Fig. 9c).

4.5.3. Body temperature monitoring

For orthopedic surgeon, body temperature is a vital signal to evaluate post-surgery condition. Every patient may have a body temperature increase after taking surgery, but sometimes it is physiologic while sometimes it is pathologic. Physiological pyrexia caused by the stress response of surgery can reach up to 87.1 % [167]. Infection is one of the most severe risk factors for poor prognosis after surgery. Once it occurs, antibiotics must be used, leading to increased drug resistance. When 39.5 °C ≥ body temperature ≥ 38 °C, it is defined as pyrexia, which is caused by noninfectious factors such as drug reactions and stress responses. And for high pyrexia (body temperature ≥39.5 °C) is generally caused by infection factors [168]. In addition, with the pandemic of Covid-19, body temperature monitoring is getting more and more important in clinic [169]. In 2012, Yang et al. first demonstrated the application of PyNG in temperature detection. Lead zirconate titanate (PZT) packaged with PDMS as the pyroelectric material (Fig. 10a). It can detect a minimum temperature change of 0.4 K [170]. However, PyNGs mainly detect temperature variation instead of static temperature. Karmakar et al. developed a paper-based TENG. MoS_2 and graphite are selected as dielectric materials. When temperature and weight range from 293 to 323 K and 50–72 kg respectively, output has a linear relationship with the temperature and weight changing (Fig. 10b) [171]. Rao et al. designed a temperature and pressure detection e-skin based on TENG (Fig. 10c). It was a three-layer structured single-electrode TENG.

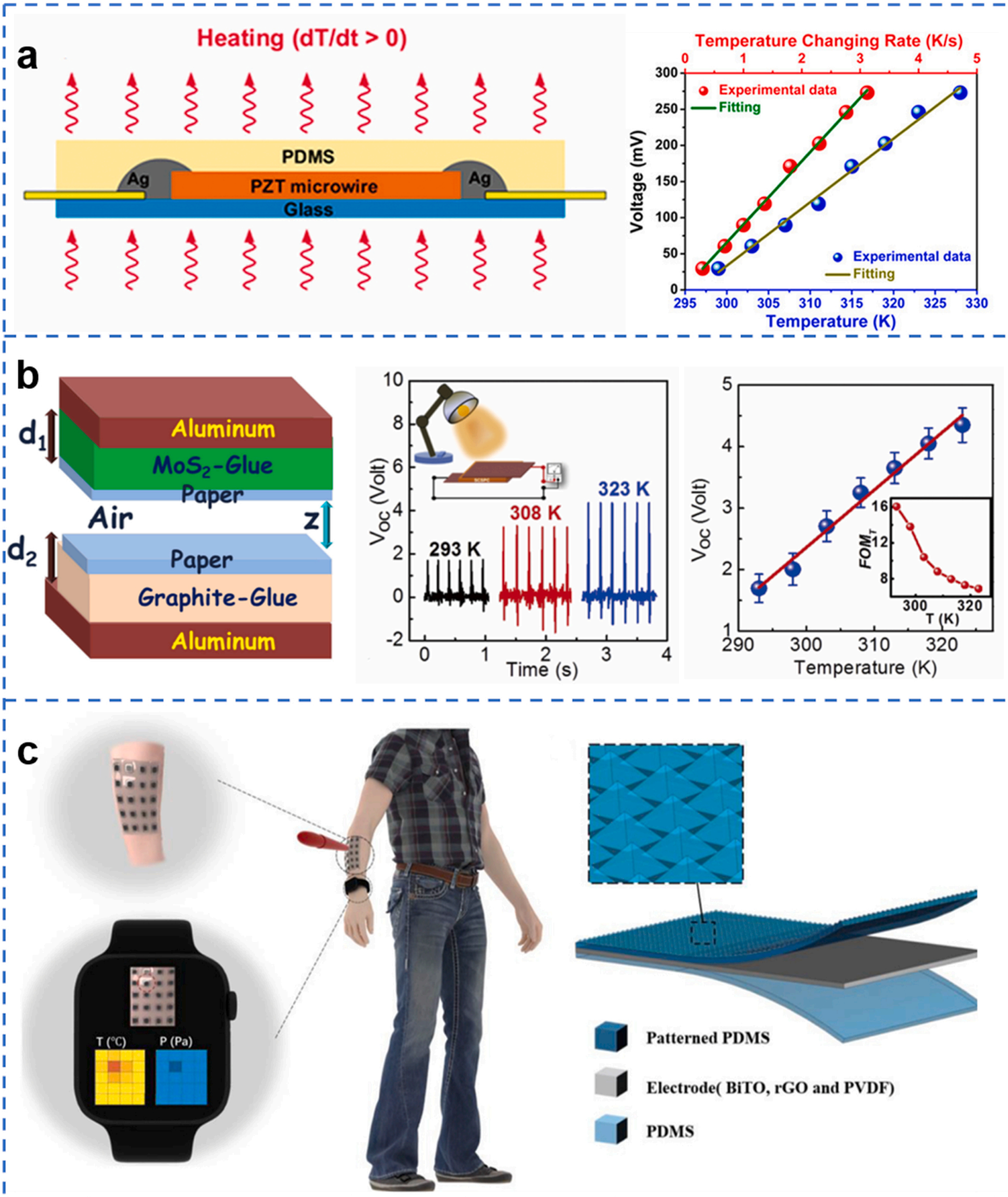

Fig. 10. NGs for temperature monitoring. (a) PyNG for temperature detection. Reprinted with permission [170]. Copyright 2012, American Chemical Society. (b) paper-based TENG for temperature detection. Reprinted with permission [171]. Copyright 2019, Elsevier Ltd. (c) Tactile electronic skin for simultaneously temperature and pressure sensing. Reprinted with permission [172]. Copyright 2020, Elsevier Ltd.

PDMS with a pyramidal microstructured surface was applied as one of the triboelectric layers on the top, which can increase the pressure sensing sensitivity. The middle layer combined rGO, $Bi_4Ti_3O_{12}$ (BiTO) served as the thermosensitive electrode. The combination of BiTO and rGO provided the TENG with good temperature sensing performance and flexibility. With the change of pressure, output voltage changed relatively with excellent sensitivity (5.07 mV/Pa). Furthermore, with the change in temperature, the electrode resistance also changed temperature (coefficient of resistance: 1.15 $\% K^{-1}$ at 25 °C, range: 25–100 °C). Both pressure sensing and temperature sensing performance were stable with the varying of each other. When attached to the skin, it can distinguish both temperature and pressure signals without interference [172].

5. Conclusions and perspectives

Orthopedics is one of the most important branches of medicine. Although surgery has a good effect on orthopedics diseases, early diagnosis can help patients avoid an invasive and painful experience. However, it is hard for individuals to do physical examinations regularly, which caused the delay of early diagnosis and treatment timing. In addition, both non-surgical and surgical treatment need a sufficiency rehabilitation approach to enable recovery [173]. Customized rehabilitation is very valid in enhancing recovery. But customized rehabilitation plans should be guided by professionals according to individual parameters, which is inconvenient to adjust in time. With the progression of nanogenerators, various of self-powered wearable devices for biosensing have been developed. Compared with traditional wearable devices, these devices are smaller, more flexible, and most important, the self-powered property provides them with a more application prospect. (Fig. 11).

i. Challenge from complex local mechanics. Wearable devices based TENG and PENG generate different amplitude of electrical output from the alterations in local mechanical behavior. Electrical output can both act as a power source to drive electronics and as an indicator to display relevant bio-signals. In current orthopedic monitoring, nanogenerators are often limited to simple mechanical scenarios, such as knees and fingers, which have a smaller ROM, and only flexion and extension functions are required. However, in clinic practice, when faced with a more complex mechanical environment, it is a struggle for NGs to meet the monitoring demand. For example, for monitoring joints with greater mobility (shoulder and elbow) and for diseases with complicated pathological mechanical alternation (scoliosis), force generates from different planes and is hard to clarify by NGs. Facing this challenge, multi-sensor integration is a promising solution for signal integration and realization of comprehensive monitoring. Meanwhile, the single indicator is not enough for diagnosis. Integrating multiple sensors can provide a comprehensive diagnosis for diseases.
ii. Large individual differences. In clinic, physicians have to deal with various types of patients. Therefore, the adoption of each indicator should avoid the influence basic factors (age, gender). In orthopedics, the mechanical discrepancy due to individual differences cannot be avoided, which significantly influence the output of NGs. Therefore, cooperation between physicians and researchers should be improved. The relationship between fundamental physiological indicators (age, gender, height, weight) and bio-signals is needed to be built by multi-data acquisition, sample size enlargement, machine learning and setting database.
iii. The contradiction between accuracy and flexibility. In medical field, accuracy of devices is important as each indictor is used to guide clinical treatment. For wearable demand, flexibility is closely related to the quality of life [174]. Therefore, it is essential to find a balance between accuracy and flexibility. The introduction of innovative materials or structure can increase the accuracy to some degree. In addition, by integrating with assistive devices or clothes, like exoskeleton, [175]. the integration of monitoring and intervention can be achieved without affecting the quality of life.
iv. Challenge from detecting signals to bio-signals. The detecting signal can be converted into multiple bio-signals by specific algorithms. Arterial pulsatility-induced electrical signals have been converted into different bio-signals including pulse, heart rate, blood pressure [176]. However, the signal conversion is uncommon in the applications of orthopedics. For example, muscle signals detected by NGs are the contraction and relaxation of a given site (mostly at the upper arm). From detected signals, muscle function indicators including muscle mass, tone, and strength are needed to be generated. Therefore, corresponding algorithmic should be developed or optimized to build a relationship between detecting signals and physical characteristics.

Fig. 11. Wearable NGs and theirs applications in orthopedics.

CRediT authorship contribution statement

Z, Li and Y, Li conceived the project. D. Yu and Z, Li searched the database, reviewed the literature and wrote the article. W, Xie helped in revising the manuscript. D. Li assisted in searching the database. All authors discussed and reviewed the manuscript.

Declaration of Competing Interest

The authors declare that they have no known competing financial interests or personal relationships that could have appeared to influence the work reported in this paper.

Data Availability

Data will be made available on request.

Acknowledgements

National Natural Science Foundation of China (61875015, 81874030, 82072506, T2125003), the Strategic Priority Research Program of the Chinese Academy of Sciences (XDA16021101), the Beijing Natural Science Foundation (JQ20038, L212010, 7224368), Hunan Yong Talents of Science and Technology (2021RC3025), Provincial Clinical Medical Technology Innovation Project of Hunan (2020SK53709), the Hunan Provincial Innovation Foundation for Postgraduate (QL20210072), Postgraduate Innovative Project of Central South University (2021XQLH041), China Postdoctoral Science Foundation (2022T150052).

References

[1] L.M. Gehrig, Orthopedic surgery, Am. J. Surg. 202 (2011) 364–368, https://doi.org/10.1016/j.amjsurg.2011.06.007.

[2] I. Lantto, J. Heikkinen, T. Flinkkila, P. Ohtonen, P. Siira, V. Laine, J. Leppilahti, A prospective randomized trial comparing surgical and nonsurgical treatments of acute achilles tendon ruptures, Am. J. Sport Med. 44 (2016) 2406–2414, https://doi.org/10.1177/0363546516651060.

[3] R.R. Bannuru, M.C. Osani, E.E. Vaysbrot, N.K. Arden, K. Bennell, S.M.A. Bierma-Zeinstra, V.B. Kraus, L.S. Lohmander, J.H. Abbott, M. Bhandari, F.J. Blanco, R. Espinosa, I.K. Haugen, J. Lin, L.A. Mandl, E. Moilanen, N. Nakamura, L. Snyder-Mackler, T. Trojian, M. Underwood, T.E. McAlindon, OARSI guidelines for the non-surgical management of knee, hip, and polyarticular osteoarthritis, Osteoarthr. Cartil. 27 (2019) 1578–1589, https://doi.org/10.1016/j.joca.2019.06.011.

[4] J. Diong, N. Allen, C. Sherrington, Structured exercise improves mobility after hip fracture: a meta-analysis with meta-regression, Br. J. Sport Med. 50 (2016) 346–355, https://doi.org/10.1136/bjsports-2014-094465.

[5] F. Landi, E. Marzetti, A.M. Martone, R. Bernabei, G. Onder, Exercise as a remedy for sarcopenia, Curr. Opin. Clin. Nutr. 17 (2014) 25–31, https://doi.org/10.1097/mco.0000000000000018.

[6] H. Hofstede, H.A.M. van der Burg, B.C. Mulder, A.M. Bohnen, P.J.E. Bindels, N. J. de Wit, E.I.T. de Schepper, S.F. van Vugt, Reducing unnecessary vitamin testing in general practice: barriers and facilitators according to general practitioners and patients, BMJ Open 9 (2019), e029760, https://doi.org/10.1136/bmjopen-2019-029760.

[7] F. Sadoughi, A. Behmanesh, N. Sayfouri, Internet of things in medicine: a systematic mapping study, J. Biomed. Inf. 103 (2020), 103383, https://doi.org/10.1016/j.jbi.2020.103383.

[8] J. Kim, A.S. Campbell, B.E. de Avila, J. Wang, Wearable biosensors for healthcare monitoring, Nat. Biotechnol. 37 (2019) 389–406, https://doi.org/10.1038/s41587-019-0045-y.

[9] J.M. Pevnick, K. Birkeland, R. Zimmer, Y. Elad, I. Kedan, Wearable technology for cardiology: An update and framework for the future, Trends Cardiovasc. Med. 28 (2018) 144–150, https://doi.org/10.1016/j.tcm.2017.08.003.

[10] J. Dai, L. Li, B. Shi, Z. Li, Recent progress of self-powered respiration monitoring systems, Biosens. Bioelectron. 194 (2021), 113609, https://doi.org/10.1016/j.bios.2021.113609.

[11] Z.L. Wang, Entropy theory of distributed energy for internet of things, Nano Energy 58 (2019) 669–672, https://doi.org/10.1016/j.nanoen.2019.02.012.

[12] Y. Hu, X. Li, Z. Zhao, C. Zhang, L. Zhou, Y. Li, Y. Liu, J. Wang, Z.L. Wang, Triboelectric nanogenerator with low crest factor via precise phase difference design realized by 3D printing, Small Methods 5 (2021) 2100936, https://doi.org/10.1002/smtd.202100936.

[13] Z.L. Wang, Triboelectric nanogenerators as new energy technology for self-powered systems and as active mechanical and chemical sensors, ACS Nano 7 (2013) 9533–9557, https://doi.org/10.1021/nn404614z.

[14] M. Wang, J. Zhang, Y. Tang, J. Li, B. Zhang, E. Liang, Y. Mao, X. Wang, Air-flow-driven triboelectric nanogenerators for self-powered real-time respiratory monitoring, ACS Nano 12 (2018) 6156–6162, https://doi.org/10.1021/acsnano.8b02562.

[15] Y. Wu, Y. Li, Y. Zou, W. Rao, Y. Gai, J. Xue, L. Wu, X. Qu, Y. Liu, G. Xu, L. Xu, Z. Liu, Z. Li, A multi-mode triboelectric nanogenerator for energy harvesting and biomedical monitoring, Nano Energy 92 (2022), https://doi.org/10.1016/j.nanoen.2021.106715.

[16] Z. Wang, J. An, J. Nie, J. Luo, J. Shao, T. Jiang, B. Chen, W. Tang, Z.L. Wang, A self-powered angle sensor at nanoradian-resolution for robotic arms and personalized medicare, Adv. Mater. 32 (2020), e2001466, https://doi.org/10.1002/adma.202001466.

[17] M. Du, Y. Cao, X. Qu, J. Xue, W. Zhang, X. Pu, B. Shi, Z. Li, Hybrid nanogenerator for biomechanical energy harvesting, motion state detection, and pulse sensing, Adv. Mater. Technol. (2022), https://doi.org/10.1002/admt.202101332.

[18] B. Wang, G. Li, Q. Zhu, W. Liu, W. Ke, W. Hua, Y. Zhou, X. Zeng, X. Sun, Z. Wen, C. Yang, Y. Pan, Bone repairment via mechanosensation of piezo1 using wearable pulsed triboelectric nanogenerator, Small (2022), e2201056, https://doi.org/10.1002/smll.202201056.

[19] Y. Yang, L. Xu, D. Jiang, B.Z. Chen, R. Luo, Z. Liu, X. Qu, C. Wang, Y. Shan, Y. Cui, H. Zheng, Z. Wang, Z.L. Wang, X.D. Guo, Z. Li, Self-powered controllable transdermal drug delivery system, Adv. Funct. Mater. (2021), https://doi.org/10.1002/adfm.202104092.

[20] D. Yang, Y. Ni, X. Kong, S. Li, X. Chen, L. Zhang, Z.L. Wang, Self-healing and elastic triboelectric nanogenerators for muscle motion monitoring and photothermal treatment, ACS Nano (2021), https://doi.org/10.1021/acsnano.1c04384.

[21] J. Rao, Z. Chen, D. Zhao, Y. Yin, X. Wang, F. Yi, Recent progress in self-powered skin sensors, Senors 19 (2019), https://doi.org/10.3390/s19122763.

[22] Z.L. Wang, From contact-electrification to triboelectric nanogenerators, Rep. Prog. Phys. (2021), https://doi.org/10.1088/1361-6633/ac0a50.

[23] F.R. Fan, L. Lin, G. Zhu, W.Z. Wu, R. Zhang, Z.L. Wang, Transparent triboelectric nanogenerators and self-powered pressure sensors based on micropatterned plastic films, Nano Lett. 12 (2012) 3109–3114, https://doi.org/10.1021/nl300988z.

[24] Z.L. Wang, Triboelectric nanogenerators as new energy technology and self-powered sensors - principles, problems and perspectives, Faraday Discuss. 176 (2014) 447–458, https://doi.org/10.1039/c4fd00159a.

[25] G. Zhu, C. Pan, W. Guo, C.Y. Chen, Y. Zhou, R. Yu, Z.L. Wang, Triboelectric-generator-driven pulse electrodeposition for micropatterning, Nano Lett. 12 (2012) 4960–4965, https://doi.org/10.1021/nl302560k.

[26] S. Wang, L. Lin, Y. Xie, Q. Jing, S. Niu, Z.L. Wang, Sliding-triboelectric nanogenerators based on in-plane charge-separation mechanism, Nano Lett. 13 (2013) 2226–2233, https://doi.org/10.1021/nl400738p.

[27] G. Zhu, Y.S. Zhou, P. Bai, X.S. Meng, Q. Jing, J. Chen, Z.L. Wang, A shape-adaptive thin-film-based approach for 50 % high-efficiency energy generation through micro-grating sliding electrification, Adv. Mater. 26 (2014) 3788–3796, https://doi.org/10.1002/adma.201400021.

[28] G. Zhu, J. Chen, Y. Liu, P. Bai, Y.S. Zhou, Q. Jing, C. Pan, Z.L. Wang, Linear-grating triboelectric generator based on sliding electrification, Nano Lett. 13 (2013) 2282–2289, https://doi.org/10.1021/nl4008985.

[29] Q.S. Jing, G. Zhu, P. Bai, Y.N. Xie, J. Chen, R.P.S. Han, Z.L. Wang, Case-encapsulated triboelectric nanogenerator for harvesting energy from reciprocating sliding motion, ACS Nano 8 (2014) 3836–3842, https://doi.org/10.1021/nn500694y.

[30] Y. Yang, Y.S. Zhou, H. Zhang, Y. Liu, S. Lee, Z.L. Wang, A single-electrode based triboelectric nanogenerator as self-powered tracking system, Adv. Mater. 25 (2013) 6594–6601, https://doi.org/10.1002/adma.201302453.

[31] S. Ankanahalli Shankaregowda, R.F. Sagade Muktar Ahmed, C.B. Nanjegowda, J. Wang, S. Guan, M. Puttaswamy, A. Amini, Y. Zhang, D. Kong, K. Sannathammegowda, F. Wang, C. Cheng, Single-electrode triboelectric nanogenerator based on economical graphite coated paper for harvesting waste environmental energy, Nano Energy 66 (2019), https://doi.org/10.1016/j.nanoen.2019.104141.

[32] H. Guo, X. Jia, L. Liu, X. Cao, N. Wang, Z.L. Wang, Freestanding triboelectric nanogenerator enables noncontact motion-tracking and positioning, ACS Nano 12 (2018) 3461–3467, https://doi.org/10.1021/acsnano.8b00140.

[33] L. Lin, Y.N. Xie, S.M. Niu, S.H. Wang, P.K. Yang, Z.L. Wang, Robust triboelectric nanogenerator based on rolling electrification and electrostatic induction at an instantaneous energy conversion efficiency of similar to 55 %, ACS Nano 9 (2015) 922–930, https://doi.org/10.1021/nn506673x.

[34] G. Zhu, J. Chen, T.J. Zhang, Q.S. Jing, Z.L. Wang, Radial-arrayed rotary electrification for high performance triboelectric generator, Nat. Commun. 5 (2014), https://doi.org/10.1038/ncomms4426.

[35] Y.N. Xie, S.H. Wang, S.M. Niu, L. Lin, Q.S. Jing, J. Yang, Z.Y. Wu, Z.L. Wang, Grating-structured freestanding triboelectric-layer nanogenerator for harvesting mechanical energy at 85 % total conversion efficiency, Adv. Mater. 26 (2014) 6599–6607, https://doi.org/10.1002/adma.201402428.

[36] S.M. Niu, Y. Liu, X.Y. Chen, S.H. Wang, Y.S. Zhou, L. Lin, Y.N. Xie, Z.L. Wang, Theory of freestanding triboelectric-layer-based nanogenerators, Nano Energy 12 (2015) 760–774, https://doi.org/10.1016/j.nanoen.2015.01.013.

[37] Z. Liu, H. Li, B. Shi, Y. Fan, Z.L. Wang, Z. Li, Wearable and implantable triboelectric nanogenerators, Adv. Funct. Mater. 29 (2019), https://doi.org/10.1002/adfm.201808820.

[38] D.J. Jiang, B.J. Shi, H. Ouyang, Y.B. Fan, Z.L. Wang, Z. Li, Emerging implantable energy harvesters and self-powered implantable medical electronics, ACS Nano 14 (2020) 6436–6448, https://doi.org/10.1021/acsnano.9b08268.

[39] Z. Zhang, J. Zhang, H. Zhang, H. Wang, Z. Hu, W. Xuan, S. Dong, J. Luo, A portable triboelectric nanogenerator for real-time respiration monitoring, Nanoscale Res. Lett. 14 (2019) 354, https://doi.org/10.1186/s11671-019-3187-4.

[40] W. Zhang, Q. Liu, S. Chao, R. Liu, X. Cui, Y. Sun, H. Ouyang, Z. Li, Ultrathin stretchable triboelectric nanogenerators improved by postcharging electrode material, ACS Appl. Mater. Interfaces 13 (2021) 42966–42976, https://doi.org/10.1021/acsami.1c13840.

[41] C. Li, D. Liu, C. Xu, Z. Wang, S. Shu, Z. Sun, W. Tang, Z.L. Wang, Sensing of joint and spinal bending or stretching via a retractable and wearable badge reel, Nat. Commun. 12 (2021) 2950, https://doi.org/10.1038/s41467-021-23207-8.

[42] Z.L. Wang, J. Song, Piezoelectric nanogenerators based on zinc oxide nanowire arrays, Science 312 (2006) 242–246, https://doi.org/10.1126/science.1124005.

[43] Y. Hu, Y. Zhang, C. Xu, G. Zhu, Z.L. Wang, High-output nanogenerator by rational unipolar assembly of conical nanowires and its application for driving a small liquid crystal display, Nano Lett. 10 (2010) 5025–5031, https://doi.org/10.1021/nl103203u.

[44] P. Martins, A.C. Lopes, S. Lanceros-Mendez, Electroactive phases of poly (vinylidene fluoride): determination, processing and applications, Prog. Polym. Sci. 39 (2014) 683–706, https://doi.org/10.1016/j.progpolymsci.2013.07.006.

[45] S.B. Lang, S. Muensit, Review of some lesser-known applications of piezoelectric and pyroelectric polymers, Appl. Phys. A-Mater. 85 (2006) 125–134, https://doi.org/10.1007/s00339-006-3688-8.

[46] W.F. Liu, X.B. Ren, Large piezoelectric effect in Pb-free ceramics, Phys. Rev. Lett. 103 (2009), https://doi.org/10.1103/PhysRevLett.103.257602.

[47] D. Damjanovic, Contributions to the piezoelectric effect in ferroelectric single crystals and ceramics, J. Am. Ceram. Soc. 88 (2005) 2663–2676, https://doi.org/10.1111/j.1551-2916.2005.00671.x.

[48] D. Kim, S.A. Han, J.H. Kim, J.H. Lee, S.W. Kim, S.W. Lee, Biomolecular piezoelectric materials: from amino acids to living tissues, Adv. Mater. 32 (2020), e1906989, https://doi.org/10.1002/adma.201906989.

[49] R.A. Surmenev, T. Orlova, R.V. Chernozem, A.A. Ivanova, A. Bartasyte, S. Mathur, M.A. Surmeneva, Hybrid lead-free polymer-based nanocomposites with improved piezoelectric response for biomedical energy-harvesting applications: a review, Nano Energy 62 (2019) 475–506, https://doi.org/10.1016/j.nanoen.2019.04.090.

[50] L. Li, W.D. Liu, Q. Liu, Z.G. Chen, Multifunctional wearable thermoelectrics for personal thermal management, Adv. Funct. Mater. 32 (2022), https://doi.org/10.1002/adfm.202200548.
[51] G.-K. Ren, J.-L. Lan, L.-D. Zhao, C. Liu, H. Yuan, Y. Shi, Z. Zhou, Y.-H. Lin, Layered oxygen-containing thermoelectric materials: mechanisms, strategies, and beyond, Mater. Today 29 (2019) 68–85, https://doi.org/10.1016/j.mattod.2019.07.003.
[52] Z.-G. Chen, W.-D. Liu, Thermoelectric coolers: Infinite potentials for finite localized microchip cooling, J. Mater. Sci. Technol. 121 (2022) 256–262, https://doi.org/10.1016/j.jmst.2021.12.069.
[53] B. Hu, X.-L. Shi, J. Zou, Z.-G. Chen, Thermoelectrics for medical applications: progress, challenges, and perspectives, Chem. Eng. J. 437 (2022), https://doi.org/10.1016/j.cej.2022.135268.
[54] X. Li, S.-G. Lu, X.-Z. Chen, H. Gu, X.-S. Qian, Q.M. Zhang, Pyroelectric and electrocaloric materials, J. Mater. Chem. C 1 (2013) 23–37, https://doi.org/10.1039/c2tc00283c.
[55] C.R. Bowen, J. Taylor, E. LeBoulbar, D. Zabek, A. Chauhan, R. Vaish, Pyroelectric materials and devices for energy harvesting applications, Energy Environ. Sci. 7 (2014) 3836–3856, https://doi.org/10.1039/c4ee01759e.
[56] Y. Yang, W. Guo, K.C. Pradel, G. Zhu, Y. Zhou, Y. Zhang, Y. Hu, L. Lin, Z.L. Wang, Pyroelectric nanogenerators for harvesting thermoelectric energy, Nano Lett. 12 (2012) 2833–2838, https://doi.org/10.1021/nl3003039.
[57] H.H. Singh, N. Khare, Flexible ZnO-PVDF/PTFE based piezo-tribo hybrid nanogenerator, Nano Energy 51 (2018) 216–222, https://doi.org/10.1016/j.nanoen.2018.06.055.
[58] J.H. Lee, K.Y. Lee, M.K. Gupta, T.Y. Kim, D.Y. Lee, J. Oh, C. Ryu, W.J. Yoo, C. Y. Kang, S.J. Yoon, J.B. Yoo, S.W. Kim, Highly stretchable piezoelectric-pyroelectric hybrid nanogenerator, Adv. Mater. 26 (2014) 765–769, https://doi.org/10.1002/adma.201303570.
[59] Y. Zi, L. Lin, J. Wang, S. Wang, J. Chen, X. Fan, P.-K. Yang, F. Yi, Z.L. Wang, Triboelectric–pyroelectric–piezoelectric hybrid cell for high-efficiency energy-harvesting and self-powered sensing, Adv. Mater. 27 (2015) 2340–2347, https://doi.org/10.1002/adma.201500121.
[60] Z. Wang, A.K. Wann, C.L. Thompson, A. Hassen, W. Wang, M.M. Knight, IFT88 influences chondrocyte actin organization and biomechanics, Osteoarthr. Cartil. 24 (2016) 544–554, https://doi.org/10.1016/j.joca.2015.10.003.
[61] T. Quan, Z.L. Wang, Y. Yang, A shared-electrode-based hybridized electromagnetic-triboelectric nanogenerator, ACS Appl. Mater. Interfaces 8 (2016) 19573–19578, https://doi.org/10.1021/acsami.6b07162.
[62] H. Li, X. Zhang, L.M. Zhao, D.J. Jiang, L.L. Xu, Z. Liu, Y.X. Wu, K. Hu, M.R. Zhang, J.X. Wang, Y.B. Fan, Z. Li, A hybrid biofuel and triboelectric nanogenerator for bioenergy harvesting, Nano-Micro Lett. 12 (2020), https://doi.org/10.1007/s40820-020-0376-8.
[63] R. Cao, J.N. Wang, Y. Xing, W.X. Song, N.W. Li, S.Y. Zhao, C. Zhang, C.J. Li, A self-powered lantern based on a triboelectric-photovoltaic hybrid nanogenerator, Adv. Mater. Technol. 3 (2018), https://doi.org/10.1002/admt.201700371.
[64] K. Dong, X. Peng, Z.L. Wang, Fiber/fabric-based piezoelectric and triboelectric nanogenerators for flexible/stretchable and wearable electronics and artificial intelligence, Adv. Mater. 32 (2020), e1902549, https://doi.org/10.1002/adma.201902549.
[65] X. Pu, L. Li, H. Song, C. Du, Z. Zhao, C. Jiang, G. Cao, W. Hu, Z.L. Wang, A self-charging power unit by integration of a textile triboelectric nanogenerator and a flexible lithium-ion battery for wearable electronics, Adv. Mater. 27 (2015) 2472–2478, https://doi.org/10.1002/adma.201500311.
[66] T. Zhou, C. Zhang, C.B. Han, F.R. Fan, W. Tang, Z.L. Wang, Woven structured triboelectric nanogenerator for wearable devices, ACS Appl. Mater. Interfaces 6 (2014) 14695–14701, https://doi.org/10.1021/am504110u.
[67] K.N. Kim, J. Chun, J.W. Kim, K.Y. Lee, J.U. Park, S.W. Kim, Z.L. Wang, J.M. Baik, Highly stretchable 2D fabrics for wearable triboelectric nanogenerator under harsh environments, ACS Nano 9 (2015) 6394–6400, https://doi.org/10.1021/acsnano.5b02010.
[68] K. Dong, J. Deng, W. Ding, A.C. Wang, P. Wang, C. Cheng, Y.-C. Wang, L. Jin, B. Gu, B. Sun, Z.L. Wang, Versatile core-sheath yarn for sustainable biomechanical energy harvesting and real-time human-interactive sensing, Adv. Energy Mater. 8 (2018), https://doi.org/10.1002/aenm.201801114.
[69] K. Dong, J. Deng, W. Ding, A.C. Wang, P. Wang, C. Cheng, Y.-C. Wang, L. Jin, B. Gu, B. Sun, Z.L. Wang, Versatile core–sheath yarn for sustainable biomechanical energy harvesting and real-time human-interactive sensing, Adv. Energy Mater. 8 (2018) 1801114, https://doi.org/10.1002/aenm.201801114.
[70] L. Ma, R. Wu, A. Patil, J. Yi, D. Liu, X. Fan, F. Sheng, Y. Zhang, S. Liu, S. Shen, J. Wang, Z.L. Wang, Acid and alkali-resistant textile triboelectric nanogenerator as a smart protective suit for liquid energy harvesting and self-powered monitoring in high-risk environments, Adv. Funct. Mater. 31 (2021) 2102963, https://doi.org/10.1002/adfm.202102963.
[71] Z. Wang, Z. Ruan, W.S. Ng, H. Li, Z. Tang, Z. Liu, Y. Wang, H. Hu, C. Zhi, Integrating a triboelectric nanogenerator and a zinc-ion battery on a designed flexible 3D spacer fabric, Small Methods 2 (2018) 1800150, https://doi.org/10.1002/smtd.201800150.
[72] K. Xia, D. Wu, J. Fu, N.A. Hoque, Y. Ye, Z. Xu, A high-output triboelectric nanogenerator based on nickel–copper bimetallic hydroxide nanowrinkles for self-powered wearable electronics, J. Mater. Chem. A 8 (2020) 25995–26003, https://doi.org/10.1039/d0ta09440d.
[73] J. Xiong, P. Cui, X. Chen, J. Wang, K. Parida, M.F. Lin, P.S. Lee, Skin-touch-actuated textile-based triboelectric nanogenerator with black phosphorus for durable biomechanical energy harvesting, Nat. Commun. 9 (2018) 4280, https://doi.org/10.1038/s41467-018-06759-0.
[74] Y. Qian, M. Sohn, W. He, H. Park, K.R.V. Subramanian, D.J. Kang, A high-output flexible triboelectric nanogenerator based on polydimethylsiloxane/three-dimensional bilayer graphene/carbon cloth composites, J. Mater. Chem. A 8 (2020) 17150–17155, https://doi.org/10.1039/d0ta04341a.
[75] M. Zhu, Q. Shi, T. He, Z. Yi, Y. Ma, B. Yang, T. Chen, C. Lee, Self-powered and self-functional cotton sock using piezoelectric and triboelectric hybrid mechanism for healthcare and sports monitoring, ACS Nano 13 (2019) 1940–1952, https://doi.org/10.1021/acsnano.8b08329.
[76] F.R. Fan, W. Tang, Z.L. Wang, Flexible nanogenerators for energy harvesting and self-powered electronics, Adv. Mater. 28 (2016) 4283–4305, https://doi.org/10.1002/adma.201504299.
[77] K.I. Park, J.H. Son, G.T. Hwang, C.K. Jeong, J. Ryu, M. Koo, I. Choi, S.H. Lee, M. Byun, Z.L. Wang, K.J. Lee, Highly-efficient, flexible piezoelectric PZT thin film nanogenerator on plastic substrates, Adv. Mater. 26 (2014) 2514–2520, https://doi.org/10.1002/adma.201305659.
[78] G.-T. Hwang, J. Yang, S.H. Yang, H.-Y. Lee, M. Lee, D.Y. Park, J.H. Han, S.J. Lee, C.K. Jeong, J. Kim, K.-I. Park, K.J. Lee, A reconfigurable rectified flexible energy harvester via solid-state single crystal grown PMN-PZT, Adv. Energy Mater. 5 (2015), https://doi.org/10.1002/aenm.201500051.
[79] Y. Hong, B. Wang, W. Lin, L. Jin, S. Liu, X. Luo, J. Pan, W. Wang, Z. Yang, Highly anisotropic and flexible piezoceramic kirigami for preventing joint disorders, Sci. Adv. 7 (2021), https://doi.org/10.1126/sciadv.abf0795.
[80] Z. Pi, J. Zhang, C. Wen, Z.-B. Zhang, D. Wu, Flexible piezoelectric nanogenerator made of poly(vinylidenefluoride-co-trifluoroethylene) (PVDF-TrFE) thin film, Nano Energy 7 (2014) 33–41, https://doi.org/10.1016/j.nanoen.2014.04.016.
[81] X.L. Chen, X.M. Li, J.Y. Shao, N.L. An, H.M. Tian, C. Wang, T.Y. Han, L. Wang, B. H. Lu, High-performance piezoelectric nanogenerators with imprinted P(VDF-TrFE)/BaTiO3 nanocomposite micropillars for self-powered flexible sensors, Small 13 (2017), https://doi.org/10.1002/smll.201604245.
[82] W. Deng, T. Yang, L. Jin, C. Yan, H. Huang, X. Chu, Z. Wang, D. Xiong, G. Tian, Y. Gao, H. Zhang, W. Yang, Cowpea-structured PVDF/ZnO nanofibers based flexible self-powered piezoelectric bending motion sensor towards remote control of gestures, Nano Energy 55 (2019) 516–525, https://doi.org/10.1016/j.nanoen.2018.10.049.
[83] Y. Wang, Y. Yang, Z.L. Wang, Triboelectric nanogenerators as flexible power sources, npj Flex. Electron 1 (2017), https://doi.org/10.1038/s41528-017-0007-8.
[84] Q. Liu, Z. Chang, Z. Li, X. Zhang, Flexible metal–air batteries: progress, challenges, and perspectives, Small Methods 2 (2018) 1700231, https://doi.org/10.1002/smtd.201700231.
[85] F.-R. Fan, Z.-Q. Tian, Z. Lin Wang, Flexible triboelectric generator, Nano Energy 1 (2012) 328–334, https://doi.org/10.1016/j.nanoen.2012.01.004.
[86] Z. Jin, F. Zhao, Y. Lei, Y.-C. Wang, Hydrogel-based triboelectric devices for energy-harvesting and wearable sensing applications, Nano Energy 95 (2022), https://doi.org/10.1016/j.nanoen.2022.106988.
[87] X. Pu, M. Liu, X. Chen, J. Sun, C. Du, Y. Zhang, J. Zhai, W. Hu, Z.L. Wang, Ultrastretchable, transparent triboelectric nanogenerator as electronic skin for biomechanical energy harvesting and tactile sensing, Sci. Adv. 3 (2017), e1700015, https://doi.org/10.1126/sciadv.1700015.
[88] Y. Liu, L. Wang, L. Zhao, X. Yu, Y. Zi, Recent progress on flexible nanogenerators toward self-powered systems, InfoMat 2 (2020) 318–340, https://doi.org/10.1002/inf2.12079.
[89] Y. Zou, Y. Gai, P. Tan, D. Jiang, X. Qu, J. Xue, H. Ouyang, B. Shi, L. Li, D. Luo, Y. Deng, Z. Li, Z.L. Wang, Stretchable graded multichannel self-powered respiratory sensor inspired by shark gill, Fundam. Res. (2022), https://doi.org/10.1016/j.fmre.2022.01.003.
[90] S. Wang, Z.L. Wang, Y. Yang, A one-structure-based hybridized nanogenerator for scavenging mechanical and thermal energies by triboelectric–piezoelectric–pyroelectric effects, Adv. Mater. 28 (2016) 2881–2887, https://doi.org/10.1002/adma.201505684.
[91] Y. Luo, Z. Wang, J. Wang, X. Xiao, Q. Li, W. Ding, H.Y. Fu, Triboelectric bending sensor based smart glove towards intuitive multi-dimensional human-machine interfaces, Nano Energy 89 (2021), https://doi.org/10.1016/j.nanoen.2021.106330.
[92] Z. Liu, Q. Zheng, Y. Shi, L. Xu, Y. Zou, D. Jiang, B. Shi, X. Qu, H. Li, H. Ouyang, R. Liu, Y. Wu, Y. Fan, Z. Li, Flexible and stretchable dual mode nanogenerator for rehabilitation monitoring and information interaction, J. Mater. Chem. B 8 (2020) 3647–3654, https://doi.org/10.1039/c9tb02466b.
[93] D. Jiang, H. Ouyang, B. Shi, Y. Zou, P. Tan, X. Qu, S. Chao, Y. Xi, C. Zhao, Y. Fan, Z. Li, A wearable noncontact free-rotating hybrid nanogenerator for self-powered electronics, InfoMat 2 (2020) 1191–1200, https://doi.org/10.1002/inf2.12103.
[94] B. Zhang, Y. Tang, R. Dai, H. Wang, X. Sun, C. Qin, Z. Pan, E. Liang, Y. Mao, Breath-based human–machine interaction system using triboelectric nanogenerator, Nano Energy 64 (2019), https://doi.org/10.1016/j.nanoen.2019.103953.
[95] Y. Han, F. Yi, C. Jiang, K. Dai, Y. Xu, X. Wang, Z. You, Self-powered gait pattern-based identity recognition by a soft and stretchable triboelectric band, Nano Energy 56 (2019) 516–523, https://doi.org/10.1016/j.nanoen.2018.11.078.
[96] K. Trajanoska, J.D. Schoufour, E.A.L. de Jonge, B.C.T. Kieboom, M. Mulder, B. H. Stricker, T. Voortman, A.G. Uitterlinden, E.H.G. Oei, M.A. Ikram, M. C. Zillikens, F. Rivadeneira, L. Oei, Fracture incidence and secular trends between 1989 and 2013 in a population based cohort: The Rotterdam Study, Bone 114 (2018) 116–124, https://doi.org/10.1016/j.bone.2018.06.004.

[97] J.G. Quicke, P.G. Conaghan, N. Corp, G. Peat, Osteoarthritis year in review 2021: epidemiology & therapy, Osteoarthr. Cartil. 30 (2022) 196–206, https://doi.org/10.1016/j.joca.2021.10.003.
[98] S. Glyn-Jones, A.J.R. Palmer, R. Agricola, A.J. Price, T.L. Vincent, H. Weinans, A. J. Carr, Osteoarthritis, Lancet 386 (2015) 376–387, https://doi.org/10.1016/s0140-6736(14)60802-3.
[99] J. Martel-Pelletier, A.J. Barr, F.M. Cicuttini, P.G. Conaghan, C. Cooper, M. B. Goldring, S.R. Goldring, G. Jones, A.J. Teichtahl, J.P. Pelletier, Osteoarthritis, Nat. Rev. Dis. Prim. 2 (2016) 16072, https://doi.org/10.1038/nrdp.2016.72.
[100] Y. Kuroyanagi, T. Nagura, H. Matsumoto, T. Otani, Y. Toyama, Y. Suda, Weight-bearing flexion angle correlates significantly with severity of knee osteoarthritis, Knee 16 (2009) 371–374, https://doi.org/10.1016/j.knee.2009.01.003.
[101] S. Wang, M. He, B. Weng, L. Gan, Y. Zhao, N. Li, Y. Xie, Stretchable and wearable triboelectric nanogenerator based on kinesio tape for self-powered human motion sensing, Nanomaterials 8 (2018), https://doi.org/10.3390/nano8090657.
[102] M.J. Bade, T. Struessel, M. Dayton, J. Foran, R.H. Kim, T. Miner, P. Wolfe, W. M. Kohrt, D. Dennis, J.E. Stevens-Lapsley, Early high-intensity versus low-intensity rehabilitation after total knee arthroplasty: a randomized controlled trial, Arthrit Care Res. 69 (2017) 1360–1368, https://doi.org/10.1002/acr.23139.
[103] J. Luo, Y. Li, M. He, Z. Wang, C. Li, D. Liu, J. An, W. Xie, Y. He, W. Xiao, Z. Li, Z. L. Wang, W. Tang, Rehabilitation of total knee arthroplasty by integrating conjoint isometric myodynamia and real-time rotation sensing system, Adv. Sci. (2022), e2105219, https://doi.org/10.1002/advs.202105219.
[104] R.N. Dunn, M.Ben Husien, Spinal tuberculosis: review of current management, Bone Jt. J. 100-B (2018) 425–431, https://doi.org/10.1302/0301-620X.100B4.BJJ-2017-1040.R1.
[105] R. El-Hawary, C. Chukwunyerenwa, Update on evaluation and treatment of scoliosis, Pediatr. Clin. N. Am. 61 (2014) 1223–1241, https://doi.org/10.1016/j.pcl.2014.08.007.
[106] M. Cruz-Jimenez, Normal changes in gait and mobility problems in the elderly, Phys. Med. Rehab. Clin. N. Am. 28 (2017) 713–725, https://doi.org/10.1016/j.pmr.2017.06.005.
[107] J.M. Baker, Gait disorders, Am. J. Med. 131 (2018) 602–607, https://doi.org/10.1016/j.amjmed.2017.11.051.
[108] Z. Lin, Z. Wu, B. Zhang, Y.-C. Wang, H. Guo, G. Liu, C. Chen, Y. Chen, J. Yang, Z. L. Wang, A triboelectric nanogenerator-based smart insole for multifunctional gait monitoring, Adv. Mater. Technol. 4 (2019), https://doi.org/10.1002/admt.201800360.
[109] J.A. Barrios, K.M. Crossley, I.S. Davis, Gait retraining to reduce the knee adduction moment through real-time visual feedback of dynamic knee alignment, J. Biomech. 43 (2010) 2208–2213, https://doi.org/10.1016/j.jbiomech.2010.03.040.
[110] A. Karatsidis, R.E. Richards, J.M. Konrath, J.C. van den Noort, H.M. Schepers, G. Bellusci, J. Harlaar, P.H. Veltink, Validation of wearable visual feedback for retraining foot progression angle using inertial sensors and an augmented reality headset, J. Neuroeng. Rehabil. 15 (2018), https://doi.org/10.1186/s12984-018-0419-2.
[111] Z. Zhang, T. He, M. Zhu, Z. Sun, Q. Shi, J. Zhu, B. Dong, M.R. Yuce, C. Lee, Deep learning-enabled triboelectric smart socks for IoT-based gait analysis and VR applications, npj Flex. Electron. 4 (2020), https://doi.org/10.1038/s41528-020-00092-7.
[112] L. Allet, I.J. H, K. Meijer, P. Willems, H. Savelberg, The influence of stride-length on plantar foot-pressures and joint moments, Gait Posture 34 (2011) 300–306, https://doi.org/10.1016/j.gaitpost.2011.05.013.
[113] A.K. Buldt, S. Forghany, K.B. Landorf, P. Levinger, G.S. Murley, H.B. Menz, Foot posture is associated with plantar pressure during gait: A comparison of normal, planus and cavus feet, Gait Posture 62 (2018) 235–240, https://doi.org/10.1016/j.gaitpost.2018.03.005.
[114] E. Toullec, Adult flatfoot, Orthop. Trauma. 101 (2015) S11–S17, https://doi.org/10.1016/j.otsr.2014.07.030.
[115] N. Miura, K. Nagai, K. Tagomori, H. Ikutomo, K. Okamura, T. Okuno, N. Nakagawa, K. Masuhara, Plantar pressure distribution during standing in women with end-stage hip osteoarthritis, Gait Posture 76 (2020) 39–43, https://doi.org/10.1016/j.gaitpost.2019.10.026.
[116] E. Klimiec, K. Zaraska, J. Piekarski, P. Guzdek, G. Kolaszczynski, B. Jasiewicz, Durable sensors for measurement of foot plantar pressure with piezoelectric polyvinylidene fluoride foil, Sens. Actuators A-Phys. 247 (2016) 504–513, https://doi.org/10.1016/j.sna.2016.07.010.
[117] S. Rajala, R. Mattila, I. Kaartinen, J. Lekkala, Designing, manufacturing and testing of a piezoelectric polymer film in-sole sensor for plantar pressure distribution measurements, IEEE Sens. J. 17 (2017) 6798–6805, https://doi.org/10.1109/jsen.2017.2750241.
[118] C. Deng, W. Tang, L. Liu, B. Chen, M. Li, Z.L. Wang, Self -powered insole plantar pressure mapping system, Adv. Funct. Mater. 28 (2018), https://doi.org/10.1002/adfm.201801606.
[119] D. Liu, D. Zhang, Z. Sun, S. Zhou, W. Li, C. Li, W. Li, W. Tang, Z.L. Wang, Active-matrix sensing array assisted with machine-learning approach for lumbar degenerative disease diagnosis and postoperative assessment, Adv. Funct. Mater. (2022), https://doi.org/10.1002/adfm.202113008.
[120] Y.-T. Jao, P.-K. Yang, C.-M. Chiu, Y.-J. Lin, S.-W. Chen, D. Choi, Z.-H. Lin, A textile-based triboelectric nanogenerator with humidity-resistant output characteristic and its applications in self-powered healthcare sensors, Nano Energy 50 (2018) 513–520, https://doi.org/10.1016/j.nanoen.2018.05.071.
[121] W.R. Frontera, J. Ochala, Skeletal muscle: a brief review of structure and function, Calcif. Tissue Int. 96 (2015) 183–195, https://doi.org/10.1007/s00223-014-9915-y.
[122] T. Paillard, Relationship between muscle function, muscle typology and postural performance according to different postural conditions in young and older adults, Front. Physiol. 8 (2017) 585, https://doi.org/10.3389/fphys.2017.00585.
[123] V. Baltzopoulos, D.A. Brodie, Isokinetic dynamometry. Applications and limitations, Sports Med. 8 (1989) 101–116, https://doi.org/10.2165/00007256-198908020-00003.
[124] Z. Yang, Y. Pang, X.L. Han, Y. Yang, J. Ling, M. Jian, Y. Zhang, Y. Yang, T.L. Ren, Graphene textile strain sensor with negative resistance variation for human motion detection, ACS Nano 12 (2018) 9134–9141, https://doi.org/10.1021/acsnano.8b03391.
[125] X. Zhang, J. Wang, Y. Xing, C. Li, Woven wearable electronic textiles as self-powered intelligent tribo-sensors for activity monitoring, Glob. Chall. 3 (2019) 1900070, https://doi.org/10.1002/gch2.201900070.
[126] H. Wang, D. Li, W. Zhong, L. Xu, T. Jiang, Z.L. Wang, Self-powered inhomogeneous strain sensor enabled joint motion and three-dimensional muscle sensing, ACS Appl. Mater. Interfaces 11 (2019) 34251–34257, https://doi.org/10.1021/acsami.9b12195.
[127] C. Wang, X. Qu, Q. Zheng, Y. Liu, P. Tan, B. Shi, H. Ouyang, S. Chao, Y. Zou, C. Zhao, Z. Liu, Y. Li, Z. Li, Stretchable, self-healing, and skin-mounted active sensor for multipoint muscle function assessment, ACS Nano 15 (2021) 10130–10140, https://doi.org/10.1021/acsnano.1c02010.
[128] O. Bruyere, G. Honvo, N. Veronese, N.K. Arden, J. Branco, E.M. Curtis, N.M. Al-Daghri, G. Herrero-Beaumont, J. Martel-Pelletier, J.P. Pelletier, F. Rannou, R. Rizzoli, R. Roth, D. Uebelhart, C. Cooper, J.Y. Reginster, An updated algorithm recommendation for the management of knee osteoarthritis from the european society for clinical and economic aspects of osteoporosis, osteoarthritis and musculoskeletal diseases (ESCEO, Semin. Arthritis Rheumatol. 49 (2019) 337–350, https://doi.org/10.1016/j.semarthrit.2019.04.008.
[129] S. Ali, J.D. Pimentel, C. Ma, Naproxen-induced liver injury, Hepatob Pancreat. Dis. 10 (2011) 552–556, https://doi.org/10.1016/s1499-3872(11)60093-3.
[130] S. Harirforoosh, W. Asghar, F. Jamali, Adverse effects of nonsteroidal antiinflammatory drugs: an update of gastrointestinal, cardiovascular and renal complications, J. Pharm. Sci. 16 (2013) 821–847, https://doi.org/10.18433/j3vw2f.
[131] G. García-Rayado, M. Navarro, A. Lanas, NSAID induced gastrointestinal damage and designing GI-sparing NSAIDs, Expert Rev. Clin. Pharmacol. 11 (2018) 1031–1043, https://doi.org/10.1080/17512433.2018.1516143.
[132] Q. Ouyang, X. Feng, S. Kuang, N. Panwar, P. Song, C. Yang, G. Yang, X. Hemu, G. Zhang, H.S. Yoon, J.P. Tam, B. Liedberg, G. Zhu, K.-T. Yong, Z.L. Wang, Self-powered, on-demand transdermal drug delivery system driven by triboelectric nanogenerator, Nano Energy 62 (2019) 610–619, https://doi.org/10.1016/j.nanoen.2019.05.056.
[133] C. Wu, P. Jiang, W. Li, H. Guo, J. Wang, J. Chen, M.R. Prausnitz, Z.L. Wang, Self-powered iontophoretic transdermal drug delivery system driven and regulated by biomechanical motions, Adv. Funct. Mater. 30 (2019), https://doi.org/10.1002/adfm.201907378.
[134] Z. Liu, J. Nie, B. Miao, J. Li, Y. Cui, S. Wang, X. Zhang, G. Zhao, Y. Deng, Y. Wu, Z. Li, L. Li, Z.L. Wang, Self-powered intracellular drug delivery by a biomechanical energy-driven triboelectric nanogenerator, Adv. Mater. 31 (2019), https://doi.org/10.1002/adma.201807795.
[135] T.E. McAlindon, R.R. Bannuru, M.C. Sullivan, N.K. Arden, F. Berenbaum, S. M. Bierma-Zeinstra, G.A. Hawker, Y. Henrotin, D.J. Hunter, H. Kawaguchi, K. Kwoh, S. Lohmander, F. Rannou, E.M. Roos, M. Underwood, OARSI guidelines for the non-surgical management of knee osteoarthritis, Osteoarthr. Cartil. 22 (2014) 363–388, https://doi.org/10.1016/j.joca.2014.01.003.
[136] Y. Zhang, L. Xu, Z. Liu, X. Cui, Z. Xiang, J. Bai, D. Jiang, J. Xue, C. Wang, Y. Lin, Z. Li, Y. Shan, Y. Yang, L. Bo, Z. Li, X. Zhou, Self-powered pulsed direct current stimulation system for enhancing osteogenesis in MC3T3-E1, Nano Energy 85 (2021), https://doi.org/10.1016/j.nanoen.2021.106009.
[137] T. He, H. Wang, J. Wang, X. Tian, F. Wen, Q. Shi, J.S. Ho, C. Lee, Self-sustainable wearable textile nano-energy nano-system (NENS) for next-generation healthcare applications, Adv. Sci. 6 (2019), https://doi.org/10.1002/advs.201901437.
[138] J. Wang, H. Wang, T. He, B. He, N.V. Thakor, C. Lee, Investigation of low-current direct stimulation for rehabilitation treatment related to muscle function loss using self-powered TENG system, Adv. Sci. 6 (2019) 1900149, https://doi.org/10.1002/advs.201900149.
[139] W. Tang, J. Tian, Q. Zheng, L. Yan, J. Wang, Z. Li, Z.L. Wang, Implantable self-powered low-level laser cure system for mouse embryonic osteoblasts' proliferation and differentiation, ACS Nano 9 (2015) 7867–7873, https://doi.org/10.1021/acsnano.5b03567.
[140] S.D. Wolfsthal, Is blood pressure control necessary before surgery, Med. Clin. N. Am. 77 (1993) 349–363, https://doi.org/10.1016/s0025-7125(16)30256-5.
[141] J. Saleh, M.M. El-Othmani, K.J. Saleh, Deep vein thrombosis and pulmonary embolism considerations in orthopedic surgery, Orthop. Clin. N. Am. 48 (2017) 127–135, https://doi.org/10.1016/j.ocl.2016.12.003.
[142] E. Gozubuyuk, E. Aygun, I. Basaran, N. Canbolat, B. Cavdaroglu, T. Akgul, M. I. Buget, Effects of changes in body temperature on perioperative bleeding in

adolescent idiopathic scoliosis surgery, Ther. Hypothermia Tem. (2021), https://doi.org/10.1089/ther.2021.0016.
[143] C. Barrington-Leigh, E. Galbraith, Feasible future global scenarios for human life evaluations, Nat. Commun. 10 (2019) 161, https://doi.org/10.1038/s41467-018-08002-2.
[144] D.O. Abegunde, C.D. Mathers, T. Adam, M. Ortegon, K. Strong, The burden and costs of chronic diseases in low-income and middle-income countries, Lancet 370 (2007) 1929–1938, https://doi.org/10.1016/s0140-6736(07)61696-1.
[145] S.M. Goodman, C.R. Mackenzie, Cardiovascular risk in the rheumatic disease patient undergoing orthopedic surgery, Curr. Rheumatol. Rep. 15 (2013) 354, https://doi.org/10.1007/s11926-013-0354-y.
[146] D.Y. Park, D.J. Joe, D.H. Kim, H. Park, J.H. Han, C.K. Jeong, H. Park, J.G. Park, B. Joung, K.J. Lee, Self-powered real-time arterial pulse monitoring using ultrathin epidermal piezoelectric sensors, Adv. Mater. 29 (2017), https://doi.org/10.1002/adma.201702308.
[147] S. Chen, N. Wu, S. Lin, J. Duan, Z. Xu, Y. Pan, H. Zhang, Z. Xu, L. Huang, B. Hu, J. Zhou, Hierarchical elastomer tuned self-powered pressure sensor for wearable multifunctional cardiovascular electronics, Nano Energy 70 (2020), https://doi.org/10.1016/j.nanoen.2020.104460.
[148] Y. Zou, J. Liao, H. Ouyang, D. Jiang, C. Zhao, Z. Li, X. Qu, Z. Liu, Y. Fan, B. Shi, L. Zheng, Z. Li, A flexible self-arched biosensor based on combination of piezoelectric and triboelectric effects, Appl. Mater. Today 20 (2020), https://doi.org/10.1016/j.apmt.2020.100699.
[149] L. Xu, Z. Zhang, F. Gao, X. Zhao, X. Xun, Z. Kang, Q. Liao, Y. Zhang, Self-powered ultrasensitive pulse sensors for noninvasive multi-indicators cardiovascular monitoring, Nano Energy 81 (2021), https://doi.org/10.1016/j.nanoen.2020.105614.
[150] Y. Fang, Y. Zou, J. Xu, G. Chen, Y. Zhou, W. Deng, X. Zhao, M. Roustaei, T. K. Hsiai, J. Chen, Ambulatory cardiovascular monitoring via a machine-learning-assisted textile triboelectric sensor, Adv. Mater. 33 (2021), e2104178, https://doi.org/10.1002/adma.202104178.
[151] F. He, X. You, W. Wang, T. Bai, G. Xue, M. Ye, Recent progress in flexible microstructural pressure sensors toward human-machine interaction and healthcare applications, Small Methods 5 (2021), e2001041, https://doi.org/10.1002/smtd.202001041.
[152] P. Tan, Y. Xi, S. Chao, D. Jiang, Z. Liu, Y. Fan, Z. Li, An artificial intelligence-enhanced blood pressure monitor wristband based on piezoelectric nanogenerator, Biosensors 12 (2022), https://doi.org/10.3390/bios12040234.
[153] Y. Isobe, S. Ito, T. Matsuda, S. Iwano, A. Uchida, N. Takahashi, T. Kojima, K. Wakahara, E. Yamaguchi, Y. Hasegawa, Longitudinal changes in pulmonary function and respiratory impedance of rheumatoid arthritis, Resp. Physiol. Neurobiol. 261 (2019) 1–8, https://doi.org/10.1016/j.resp.2018.12.008.
[154] P. Mary, L. Servais, R. Vialle, Neuromuscular diseases: diagnosis and management, Orthop. Traumatol. -Sur 104 (2018) S89–s95, https://doi.org/10.1016/j.otsr.2017.04.019.
[155] L. Bigatello, A. Pesenti, Respiratory physiology for the anesthesiologist, Anesthesiology 130 (2019) 1064–1077, https://doi.org/10.1097/aln.0000000000002666.
[156] D. Wirtz, H. Kohlhof, The geriatric patient: special aspects of peri-operative management, EFORT Open Rev. 4 (2019) 240–247, https://doi.org/10.1302/2058-5241.4.180087.
[157] J.-G. Sun, T.-N. Yang, C.-Y. Wang, L.-J. Chen, A flexible transparent one-structure tribo-piezo-pyroelectric hybrid energy generator based on bio-inspired silver nanowires network for biomechanical energy harvesting and physiological monitoring, Nano Energy 48 (2018) 383–390, https://doi.org/10.1016/j.nanoen.2018.03.071.
[158] P. Vasandani, B. Gattu, J. Wu, Z.-H. Mao, W. Jia, M. Sun, Triboelectric nanogenerator using microdome-patterned PDMS as a wearable respiratory energy harvester, Adv. Mater. Technol. -Us 2 (2017), https://doi.org/10.1002/admt.201700014.
[159] H. Xue, Q. Yang, D. Wang, W. Luo, W. Wang, M. Lin, D. Liang, Q. Luo, A wearable pyroelectric nanogenerator and self-powered breathing sensor, Nano Energy 38 (2017) 147–154, https://doi.org/10.1016/j.nanoen.2017.05.056.
[160] D.Y. Wang, D.Z. Zhang, Y. Yang, Q. Mi, J.H. Zhang, L.D. Yu, Multifunctional latex/polytetrafluoroethylene-based triboelectric nanogenerator for self-powered organ-like mxene/metal-organic framework-derived CuO nanohybrid ammonia sensor, ACS Nano 15 (2021) 2911–2919, https://doi.org/10.1021/acsnano.0c09015.
[161] V. Saasa, M. Beukes, Y. Lemmer, B. Mwakikunga, Blood ketone bodies and breath acetone analysis and their correlations in type 2 diabetes mellitus, Diagnostics 9 (2019), https://doi.org/10.3390/diagnostics9040224.
[162] G. Hancock, S. Sharma, M. Galpin, D. Lunn, C. Megson, R. Peverall, G. Richmond, G.A.D. Ritchie, K.R. Owen, The correlation between breath acetone and blood betahydroxybutyrate in individuals with type 1 diabetes, J. Breath. Res 15 (2020), 017101, https://doi.org/10.1088/1752-7163/abbf37.
[163] Y. Su, T. Yang, X. Zhao, Z. Cai, G. Chen, M. Yao, K. Chen, M. Bick, J. Wang, S. Li, G. Xie, H. Tai, X. Du, Y. Jiang, J. Chen, A wireless energy transmission enabled wearable active acetone biosensor for non-invasive prediabetes diagnosis, Nano Energy 74 (2020), https://doi.org/10.1016/j.nanoen.2020.104941.
[164] E. Ekkernkamp, H.J. Kabitz, D.J. Walker, C. Schmoor, J.H. Storre, W. Windisch, M. Dreher, Minute ventilation during spontaneous breathing, high-intensity noninvasive positive pressure ventilation and intelligent volume assured pressure support in hypercapnic COPD, Copd 11 (2014) 52–58, https://doi.org/10.3109/15412555.2013.829437.
[165] H. Chen, Y. Xu, J. Zhang, W. Wu, G. Song, Self-powered flexible blood oxygen monitoring system based on a triboelectric nanogenerator, Nanomaterials 9 (2019), https://doi.org/10.3390/nano9050778.
[166] J. Allen, Photoplethysmography and its application in clinical physiological measurement, Physiol. Meas. 28 (2007) R1–R39, https://doi.org/10.1088/0967-3334/28/3/R01.
[167] B. Ashley, D.A. Spiegel, P. Cahill, D. Talwar, K.D. Baldwin, Post-operative fever in orthopaedic surgery: How effective is the 'fever workup?', J. Orthop. Surg. 25 (2017) https://doi.org/10.1177/2309499017727953.
[168] D.J. Niven, K.B. Laupland, Pyrexia: aetiology in the ICU, Crit. Care 20 (2016) 247, https://doi.org/10.1186/s13054-016-1406-2.
[169] K.N. Kunze, P.D. Fabricant, R.G. Marx, B.U. Nwachukwu, Perspectives on the impact of the COVID-19 pandemic on the sports medicine surgeon: implications for current and future care, Clin. Sports Med. 40 (2021) 213–220, https://doi.org/10.1016/j.csm.2020.08.014.
[170] Y. Yang, Y. Zhou, J.M. Wu, Z.L. Wang, Single micro/nanowire pyroelectric nanogenerators as self-powered temperature sensors, ACS Nano 6 (2012) 8456–8461, https://doi.org/10.1021/nn303414u.
[171] S. Karmakar, P. Kumbhakar, K. Maity, D. Mandal, P. Kumbhakar, Development of flexible self-charging triboelectric power cell on paper for temperature and weight sensing, Nano Energy 63 (2019), https://doi.org/10.1016/j.nanoen.2019.06.027.
[172] J. Rao, Z. Chen, D. Zhao, R. Ma, W. Yi, C. Zhang, D. Liu, X. Chen, Y. Yang, X. Wang, J. Wang, Y. Yin, X. Wang, G. Yang, F. Yi, Tactile electronic skin to simultaneously detect and distinguish between temperature and pressure based on a triboelectric nanogenerator, Nano Energy 75 (2020), https://doi.org/10.1016/j.nanoen.2020.105073.
[173] R. Geenen, C.L. Overman, R. Christensen, P. Asenlof, S. Capela, K.L. Huisinga, M. E.P. Husebo, A.J.A. Koke, Z. Paskins, I.A. Pitsillidou, C. Savel, J. Austin, A. L. Hassett, G. Severijns, M. Stoffer-Marx, J.W.S. Vlaeyen, C. Fernandez-de-Las-Penas, S.J. Ryan, S. Bergman, EULAR recommendations for the health professional's approach to pain management in inflammatory arthritis and osteoarthritis, Ann. Rheum. Dis. 77 (2018) 797–807, https://doi.org/10.1136/annrheumdis-2017-212662.
[174] J. Kim, A.S. Campbell, B.E. de Ávila, J. Wang, Wearable biosensors for healthcare monitoring, Nat. Biotechnol. 37 (2019) 389–406, https://doi.org/10.1038/s41587-019-0045-y.
[175] B. Hu, J. Xue, D. Jiang, P. Tan, Y. Wang, M. Liu, H. Yu, Y. Zou, Z. Li, Wearable exoskeleton system for energy harvesting and angle sensing based on a piezoelectric cantilever generator array, ACS Appl. Mater. Interfaces (2022), https://doi.org/10.1021/acsami.2c08757.
[176] Q. Zheng, Q. Tang, Z.L. Wang, Z. Li, Self-powered cardiovascular electronic devices and systems, Nat. Rev. Cardiol. 18 (2021) 7–21, https://doi.org/10.1038/s41569-020-0426-4.

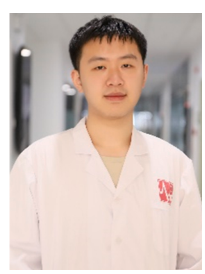

Dengjie Yu received his Bachelor of Medicine (M.D. equivalent) degree from Kunming Medical University in 2020. Then he joined the department of orthopedics, Xiangya hospital, Central South university and became a M.S. candidate. He is currently a joint student at Beijing Institute of Nanoenergy and Nanosystems, Chinese Academy of Science. His research interest is self-powered orthopedic biomedical devices and systems.

Zhe Li received her Doctor's Degree from Beijing Institute of Nanoenergy and Nanosystems, Chinese Academy of Sciences, in 2020. She is currently a post-doctoral researcher in School of Medical Technology, Institute of Engineering Medicine, Beijing Institute of Technology. Her research work is focusing on the application of nanogenerators for self-powered biomedical systems, biosensors, and biodegradable electronics.

Wenqing Xie received his Bachelor of Medicine (M.D. equivalent) degree from Northwest Minzu University in 2020. Then he joined the department of orthopedics, Xiangya hospital, Central South university and became a M.S.candidate and resident physician. His research focuses on the risk factors, pathogenesis and clinical prevention and treatment of degenerative musculoskeletal disease (osteoarthritis, sarcopenia, etc).

Daishi Li received her Bachelor of Medicine (M.D. equivalent) degree from Kinming Medical University in 2020. She joined department of dermatology, Xiangya hospital, Central South university and became a resident physician and M.S candidate. Her research focuses on melanomas immunotherapy.

Zhou Li received his Bachelor's degree from Wuhan University in 2004, and Doctor's Degree from Peking University in 2010. He joined School of Biological Science and Medical Engineering of Beihang University in 2010 as an associate Professor. Currently, he is principal investigator and group leader of Nanoenergy and Biosystem Lab (NBL) in Beijing Institute of Nanoenergy and Nanosystems, Chinese Academy of Sciences. He is supported by the National Youth Talent Support Program and the National Science Fund for Distinguished Young Scholars. His research interests include nanogenerators, in vivo energy harvesters and self-powered medical devices, biosensors.

Yusheng Li received his M.D and Ph.D. degree from Central south university in 2011, specializing in Orthopedics. From 2016–2019, he worked as a postdoctoral fellow at the department of Orthopedic surgery, Johns Hopkins university. He currently is an associate professor and associate chief physician at the department of Orthopedics, Xiangya hospital, Central South university. His research focuses on Orthopedic degenerative diseases and sports injury.